CHAMBER MEASUREMENTS OF TRACE GAS EXCHANGES FOR SEVERAL OAK SPECIES EXPOSED TO OZONE AND DROUGHT

A Thesis

by

MATTHEW RAYMOND WATSON

Submitted to the Office of Graduate and Professional Studies of
Texas A&M University
in partial fulfillment of the requirements for the degree of

MASTER OF SCIENCE

Chair of Committee,	Gunnar Schade
Committee Members,	Renyi Zhang
	David Briske
Head of Department,	Ping Yang

December 2016

Major Subject: Atmospheric Sciences

ABSTRACT

Several species of oak were used in a series of chamber based experiments. The species of oaks chosen (*Quercus alba*, *muehlenbergii*, and *virginiana*) were selected because they are all emitters of the volatile organic compound isoprene. Isoprene emissions as well as several physiological parameters such as photosynthesis and stomatal conductance were monitored under normal conditions, as well as while stressors such as drought and high external ozone were introduced. Ozone fluxes to the plants were partitioned into stomatal and surface fluxes for leaves treated with an isoprenoid coating as well as untreated leaves. It was found that the coating on the leaves acted as a strong surface ozone sink, which reduced ozone concentrations in the leaf boundary layer and resulted in significantly reduced stomatal fluxes of ozone. Measurements of drought stressed specimens displayed significant declines in photosynthesis and stomatal conductance, however isoprene emissions remained constant. This resulted in a significant increase in the percentage of assimilated carbon emitted as isoprene during times of water stress and represented a decoupling of photosynthesis from isoprene production. The level of circadian control over isoprene emissions was assessed for a *Q. muehlenbergii* specimen by exposing it to constant light for several days. No circadian control over isoprene emissions was noted for this specimen despite past research demonstrating circadian control over isoprene emissions for several other species.

DEDICATION

For Mom.

ACKNOWLEDGEMENTS

I would like to thank my committee chair and advisor, Dr. Schade, and my committee members, Dr. Zhang, and Dr. Briske, for their guidance and support throughout the course of this research.

I would like to thank all those who assisted me in the lab taking samples, building and maintaining the chamber, processing data and answering all my questions: Amanda Harte, Geoff Roest, Monica Madronich, Nora Lahr, Juan Huang, and Kevin Larson.

Thanks also go to my friends and fellow grad students, colleagues, and the department faculty and staff for making my time at Texas A&M University a great experience.

Finally, thanks to my mother and father for their encouragement.

CONTRIBUTORS AND FUNDING SOURCES

This work was supervised by a thesis committee consisting of Professor Gunnar Schade and Professor Renyi Zhang of the Department of Atmospheric Science and Professor David Briske of the Department of Ecosystem Science and Management.

All work for the thesis was completed by the student, under the advisement of Dr. Gunnar Schade of the Department of Atmospheric Science.

This work was made possible in part by the National Science Foundation (NSF) under Grant Number ATM-0955438. The content of this work is solely the responsibility of the authors and does not necessarily represent the official views of the NSF..

NOMENCLATURE

VOC	Volatile organic compound
BVOC	Biogenic volatile organic compound
IspSs	Isoprene synthase
E	Transpiration
g_s	Stomatal conductance for H_2O
A	CO_2 Assimilation
I_e	Isoprene emission
GC	Gas chromatograph
FID	Flame ionization detector
UV	Ultraviolet
IR	Infrared
STP	Standard temperature and pressure
MACR	Methacrolein
MVK	Methyl vinyl ketone
IOP	Intense observation period

TABLE OF CONTENTS

Page

LIST OF FIGURES

Page

1. INTRODUCTION

Global climate change could have profound effects on isoprene emissions and atmosphere-biosphere interactions in general; however, these effects are not fully understood. Research has shown that the changing climate will increase temperatures, elevate the severity of droughts and may locally increase the atmospheric concentrations of ozone depending on emissions of precursors (IPCC 2013 report). Increased severity of drought and atmospheric ozone will have significant negative impacts on crop yields, and because these impacts are not fully understood, it has become an important field of study (Flexas et al., 2004; Wittig et al., 2007, 2009). Ozone has been shown to damage plant structures and reduce plant productivity; however, some species of plants have the capacity to emit isoprene, which has been shown to help prevent this damage (Loreto et al. 2001; Sharkey et al., 2008). The purpose of this research is to examine the impacts of these taxing climatic conditions on the plant-atmosphere system, with a focus on isoprene emissions.

There is a need for research to determine the role that drought will play on isoprene emissions. It is understood that mild water stress has little effect on isoprene emissions; however, there is a threshold where plants become so stressed that isoprene emissions do begin to decline (Bruggemann and Schnitzler, 2002; Sharkey and Loreto, 1993; Pegoraro et al., 2004). Facing an increased occurrence of droughts due to climate change creates a need for a more complete understanding of the slope of the decline in isoprene emissions as drought incidence and severity progresses.

It is also important to improve our understanding of the interactions between ozone and isoprene because climate change projections indicate increases in isoprene and locally increased ozone (Guenther et al., 2006; IPCC 2013 report). There is also some level of uncertainty as to how ozone interacts with vegetation, in particular the partitioning between stomatal and non-stomatal ozone fluxes. There have been studies documenting the importance of both stomatal (Fares et al., 2008; Uddling et al., 2010) and non-stomatal sinks (Fares et al., 2010; Cape et al., 2009) of ozone. This work examines the relationship between stomatal and non-stomatal ozone fluxes by manipulating these fluxes. Stomatal fluxes are manipulated when plants are water stressed and stomatal conductance is restricted. A 'protective role' that drought can play in preventing ozone damage has been noted, and this work allows further examination of this relationship (Panek and Goldstein, 2001; Panek, 2004; Löw et al., 2006). Additionally, surface fluxes can be manipulated by the addition of a reactive isoprenoid coating on the leaves. This coating reduces the concentration of ozone in the leaf boundary layer, and thus reduces the stomatal ozone gradient. It is likely that this will have significant effects on the stomatal ozone flux, and the partitioning between stomatal and non-stomatal fluxes.

This work was done by monitoring gas exchanges from several species of oak in a chamber setting to evaluate their vulnerability to events such as elevated ozone and drought conditions. Oaks were chosen because many are strong emitters of the volatile organic compound isoprene. Isoprene emissions, as well as several physiological parameters such as photosynthesis and transpiration, were monitored under normal

conditions within the chamber, as well as while stressors such as drought and high external ozone were introduced.

2. LITERATURE REVIEW

2.1. Isoprene

Many species of volatile organic compounds (VOC) are emitted to the atmosphere by the biosphere, the two largest contributors to this carbon flux being methane and terpenes (isoprenoids). Biogenic methane is produced mainly by microbial activity, while most terpenes are produced by a secondary carbon metabolism in green plants (Guenther et al., 2006). Isoprene (C_5H_8; 2-methyl-1,3-butadiene), a hemiterpene, is the basic building block for all members of the isoprenoid family. Many biogenic isoprenoids have known functions: they are used as hormones (gibberellins, brassinosteroids, abscisic acid), pigments (carotenoids), and as defense against herbivory (monoterpenes, sesquiterpenes, diterpenes) by a wide range of plants and animals (Grotewold, 2006; Lange et al., 2000). Isoprene represents the largest individual emission among biogenic terpene emissions, and yet the reason for plants to produce it is not as clear as many of the less abundantly produced VOC constituents. Not all plants emit isoprene; among ferns, mosses, angiosperms and gymnosperms, there are both species that emit isoprene and species that do not (Monson et al., 2013; Sharkey et al., 2008; Hanson et al., 1999; Tingey et al., 1987). The capacity to produce isoprene requires the presence of isoprene synthase (IspSs), an enzyme necessary for the synthesis of the isoprene molecule. The gene sequence responsible for IspSs synthesis itself differs among isoprene producing species, leading to the conclusion that the capacity to produce isoprene has evolved multiple times throughout evolution (Harley et al. 1999a; Sharkey et al. 2005). Isoprene and methane each represent approximately a third of annual global

VOC emissions (both natural and anthropogenic) to the atmosphere, with the remaining third comprised of hundreds of different volatile organic compounds (Guenther et al., 2006). Global emissions of isoprene have been estimated to be 5×10^{14} g yr^{-1} (Guenther et al., 1995, 2006). Due to the large volume of these emissions and the highly reactive nature of isoprene, it plays an important role in atmospheric chemistry on a regional and global scale (Folberth et al., 2006; Dreyfus et al., 2002; Sharkey and Yeh, 2001).

Isoprene has important impacts on atmospheric chemistry for several reasons. It reacts readily with OH radicals, and because OH is responsible for removing a large portion of methane from the atmosphere, isoprene effectively increases the lifetime of atmospheric methane (Pegoraro et al., 2004, Folberth et al., 2006). In the presence of nitrogen oxides, isoprene can react to form ozone, a pollutant that has detrimental effects on human and plant health (Atkinson, 1997; Pell et al., 1997; Dreyfus et al., 2002). Isoprene forms several breakdown products including first generation methacrolein (MACR), methyl vinyl ketone (MVK), and formaldehyde (Atkinson and Arey, 2003), as well as numerous second and third generation products such as hydroxyacetone, glycolaldehyde, organic acids and nitrates, and carbon monoxide (Paulot et al., 2009). In air masses with high nitrogen oxide (NO_x) concentrations, isoprene breakdown products can also react to form peroxyacetyl nitrate (PAN) and methachrolyl-peroxyacetyl nitrate (MPAN), both of which are hazardous to human health (Williams et al., 1997). Isoprene has also been shown to lead to the growth of aerosol particles which can then act as cloud condensation nuclei (Sharkey and Yeh, 2001). Often a 'blue haze' can be seen in regions with large amounts of terpene emissions, which has been

attributed to aerosol growth due to these emissions (Glasius and Goldstein, 2016; Went, 1960).

Isoprene is produced within plant chloroplasts and is immediately released to the atmosphere (Mgaloblishvili et al., 1979; Sharkey et al., 2008). There is no known storage mechanism for isoprene as there is for certain volatile mono- and sesquiterpenes, and other biogenic volatile organic compounds (BVOC) (Sharkey et al., 2008). Because of this, it is assumed that the rate of emission is based solely on the rate of isoprene production in the plant (Sharkey and Yeh, 2001). The rate of production of isoprene depends on several factors including plant species, leaf position in the canopy (affecting long-term light exposure), ambient CO_2 concentration, incident light on the leaf, and leaf temperature (Guenther et al., 1995; Harley et al., 1999b). Research has also shown that plants eventually reduce isoprene emissions under drought conditions, likely due to reductions of precursor species in the leaves. Models of isoprene emissions have been developed and implemented to estimate emission rates, and have been scaled to estimate global production (Guenther et al., 1995, 2006; Sanderson et al., 2003; Arneth et al., 2007; Lathiere et al., 2010). While it is still unclear why plants emit isoprene, popular theories include: providing increased thermotolerance, providing protection from oxidants such as ozone, providing protection from damage associated with heat flecks, or used as an overflow mechanism for excess carbon or photosynthetic energy (Fuentes et al., 2000; Loreto et al., 2001; Singsaas and Sharkey, 1998; Sharkey, 2005; Singsaas et al., 1999; Rosenstiel et al., 2004; Sharkey and Yeh, 2001, Loreto et al., 1998).

One of the prevailing theories as to why plants produce isoprene is its role to protect leaves against heat stress. Lobell and Asner (2003) estimated up to a 17% decrease in crop yield per degree Celsius increase in average growing season temperature. Climate models project an increase in global average temperature of 1.4 - 5 °C by 2100, which could result in a significant loss in crop productivity (IPCC 2013 report). Many plants use transpirational cooling to maintain leaf temperatures, however some species with low transpiration rates, such as with oaks, experience frequent spikes in leaf temperature (Sharkey 2005). To test if isoprene can protect against heat stress, the chemical fosmidomycin, a substance shown to inhibit IspSs but not affect photosynthesis, has been used to assess isoprene's ability to mitigate heat stress damage. Sharkey et al. (2001) fed fosmidomycin to leaves and then exposed them to repeated heat spikes. These leaves showed significant reductions in photosynthesis, however when exogenous isoprene was added, the leaves displayed restored thermotolerance. Velikova and Loreto (2005) performed a similar experiment on *Phragmites australis*, and noted increased thermotolerance as well as faster recovery of photosynthesis in leaves where isoprene was not suppressed by fosmidomycin. Additionally, Penuelas et al. (2005) showed that fumigating *Quercus ilex*, a non-emitter, with isoprene resulted in significantly increased thermotolerance.

2.2. Ozone and reactive oxygen species

Another theory as to why plants produce isoprene is to protect against oxidative damage. Reactive oxygen species (ROS) are produced as a byproduct of photosynthesis under stress conditions and exist at elevated levels during times of heat stress. These

substances can damage plant structures, so plants have developed systems to scavenge them from their intercellular spaces (Wahid et al., 2007; Pell et al., 1997). Cell walls and plasma membranes in particular contain several possible sites for oxidation to occur. Cell walls contain phenolic groups, olefinic compounds and proteins, while plasma membranes are composed of proteins and unsaturated lipids, all of which provide available sites for oxidation to occur (Pell et al., 1997). Isoprene will react with ROS, and the fact that isoprene emissions respond strongly to temperature suggests that the isoprene system evolved as a method for scavenging ROS, as ROS production in leaves is also temperature dependent (Sharkey 2005; Jardine et al., 2011; Loreto et al., 2001). Plants suffer such oxidative damage when ozone enters the intercellular spaces via the stomata; this stomatal uptake of ozone can lead to the formation of the ROS hydrogen peroxide (H_2O_2), superoxide (O_2^-), and hydroxyl radical (OH). Isoprene has been shown to react with these oxidants and in turn protect the photosynthetic apparatus of the plant (Loreto et al. 2001). Ozone has been shown to damage plant structures, reduce photosynthetic production, and reduce crop yields (Pell et al., 1997; Ainsworth, 2012; Hayes et al., 2015; Wittig et al., 2007, 2009). Wittig et al. (2007) performed a meta-analysis of available studies and estimated an 11% reduction in photosynthesis measurements from trees due to ozone concentrations equal to that added since the industrial revolution. When vegetation is exposed to ozone, various plant structural parts react readily to the exposure (see above), at times creating visible damage (Loreto et al., 2001). Fluxes of ozone, typically incurring its loss, can occur to the surfaces of plant structures, to leaves' intercellular spaces via entering the stomata, or by reacting

with gaseous compounds emitted or excreted by the plant (Laisk, 1989; Cape et al., 2009; Fares et al., 2010; Jud et al., 2016).

When ozone enters the stomata and reacts with photosynthetic structures within the leaf, it has been shown to damage these structures and induce senescence (Pell et al., 1997; Miller et al., 1999; Rao and Davis 2001). Past research has documented a loss of the enzyme Rubisco as a result of ozone exposure, followed by a reduction in photosynthetic rates, and ozone-induced cell death (Pell et al., 1997; Ainsworth, 2012; Rao and Davis 2001). Non-stomatal fluxes of ozone can be either the result of surface reactions on the leaf and cuticle or gas phase reactions with emitted compounds. Several studies have pointed to a non-stomatal flux of ozone both at the ecosystem level via VOC reactions (Fares et al., 2010; Panek, 2004; Goldstein et al., 2004) and on simulated leaf surfaces (Cape et al., 2009; Jud et al., 2016). The membrane lipids of leaf surfaces are susceptible to peroxidation and denaturation when exposed to ozone and its ROS reaction products hydrogen peroxide, superoxide, and hydroxyl radical (Pell et al., 1997; Loreto et al., 2001). It has been conjectured that isoprene stabilizes membranes, and in the presence of these reactive oxygen compounds it may reduce the damage incurred by the plant (Loreto et al., 2001). Loreto et al. (2001) exposed leaves of tobacco and birch to elevated concentrations of ozone and noted significant reductions in photosynthesis and visible damage to those leaves. They then added isoprene to the gas mixture exposed to the leaves, and noted reduced declines in photosynthesis, reduced visible damage, and reduced ozone uptake by the leaf.

2.3. Circadian control

If the major reason for isoprene production is to protect against heat stress or oxidative damage, then it is likely that daily patterns of light and dark provide a selective pressure to control its production (Loivamaki et al., 2007; Johnson 2001). Several isoprene emitting species were shown to exhibit some degree of circadian control on production (Loivamaki et al., Wilkinson et al., 2006). Circadian control over a plant's physiology often provides an evolutionary advantage; many plants exhibit circadian-driven patterns in their physiology such as leaves and flowers that follow the sun or close at night (Johnson 2001). Having circadian control over isoprene production would provide an advantage because it is costly for the plant to produce, and neither heat stress nor oxidative damage typically occurs at night, making resources wasted if isoprene were produced at night (Loivamaki et al., 2007; Wilkinson et al., 2006). Because isoprene is not stored and energy is required for its production, there is little reason to expect nighttime emissions. If isoprene precursors were produced at night and IpsS operated on them, it would take energy from the plant that can't be replenished due to the lack of sunlight, possibly resulting in harm to the plant. I expected to see some degree of circadian control over isoprene emissions for these reasons.

2.4. Water stress

Water stress has profound negative effects on plant growth, stomatal conductance, and photosynthesis (Flexas et al., 2004). To preserve water within the plant, plants respond to water stress by closing their stomata. This reduces the amount of CO_2 they are able to assimilate and slows the rate of photosynthesis. In addition to

the diffusive limitations water stress has on assimilation (A) via stomatal closure, there have been metabolic limitations noted as well (Flexas et al., 2004). Under normal conditions, isoprene emission represents around 2% of recently assimilated carbon at 30 °C, but this fraction can climb to over 50% during episodes of water stress (Sharkey and Loreto, 1993; Baldocchi et al., 1995; Monson and Fall, 1989; Harley et al., 1999b; Fang et al., 1996). This is mainly caused by a reduction in assimilation as mild water stress has been shown to have a minor effect on isoprene emissions (Pegoraro et al., 2004; Sharkey and Loreto, 1993; Guenther et al., 1999). During times of severe water stress however, isoprene emissions do begin to decline rapidly. The mechanisms for this decline are either a reduction in available ATP to use in isoprene production as photosynthesis declines or a limited source of carbon (isoprene precursors) as stomata close and restrict assimilation (Sharkey and Loreto, 1993; Pegoraro et al., 2004). The fact that minor drought stress does not affect isoprene emissions presents a unique opportunity to examine the role that isoprene plays in ozone quenching for these species. Assuming that the ozone quenching to both isoprene and plant surfaces remain constant under mild water stress, then the only flux that will be affected is the stomatal flux of ozone. This will allow an examination of the role of mild drought on stomatal ozone uptake, and an assessment of a possible protective role drought may play during ozone exposure.

3. METHODS

3.1. Chamber design and sampling

For this research, a chamber in the lab was used to control and monitor the seedlings. The chamber was constructed of a cylindrical PFA Teflon foil curtain of approximately 200 L volume. The height of the chamber was adjustable to accommodate plants of different sizes and was illuminated by a ring of eight light emitting diode (LED) lamps which provided approximately 1250 μmol m^{-2} s^{-1} photosynthetically active radiation (PAR) (approximately 60% of full sun at low latitudes) to the center of the chamber. The lights were set on a timer which turned the lamps on and off at set times each day. Half the lamps were on from 7 to 10 am, followed by all the lamps on from 10 am to 4 pm, followed by half the lamps on from 4 to 7 pm. The air in the chamber was kept well mixed by a Teflon coated fan attached to the top of the chamber. The fan was mounted to a Plexiglas panel on top of the cylindrical chamber, which was lined with an additional sheet of PFA Teflon. The chamber accommodated the above-ground portion of the seedlings only, the pot containing the roots and soil remained below the chamber to allow for watering. To seal the bottom of the chamber, the Teflon curtain was gathered around the stem of the seedlings and held in place using zip ties. This eliminated the impacts of any soil activity in the chamber such as soil respiration, evaporation, nitrification, or denitrification processes. Nitrification and denitrification in particular could have introduced high concentrations of reactive nitrogen species into the chamber which could have affected VOCs chemistry in the chamber (Fowler et al., 2013).

Several holes were drilled into the top plate of the chamber to allow for sensors to be inserted. The chamber did not need to be sealed perfectly, as it was kept at a positive pressure relative to the laboratory air so any leaks typically represented air exiting, not entering the chamber. This ensured that the air sampled from the chamber was not contaminated by outside air. The flow into the chamber was flow controlled (Gilmont Industries flow meter with needle valve) at 30 L min^{-1}. Incoming flows of 40 and 50 L min^{-1} yielded e-folding residence times within the chamber of 7.6 and 9 minutes, respectively. These were measured repeatedly using decay rates of CO and CO_2 concentrations after injecting pulses of each gas. The flow into the chamber came from the house compressed air supply, introduced via Teflon tubing, and was scrubbed of particulates and low volatility carbon trace gases by passing through an activated charcoal filter cartridge. Past the cartridge, the incoming air was humidified to a specified level using an FC100 series Nafion humidifier (Perma pure LLC) fed with DI-water from a temperature-controllable circulator (HAAKE W19 D1) to maintain constant absolute humidity entering the chamber. When needed, ozone was added to the incoming air using an ultraviolet (UV) ozone generator (UVP LLC). Ozone concentrations of greater than 100 ppb within the chamber were obtainable with this generator when feeding high oxygen concentrations from an O_2-concentrator into its UV-C exposure tube.

To monitor rates of CO_2 assimilation, transpiration and ozone uptake by the plant, it was necessary to monitor the CO_2, water vapor, and ozone concentrations entering and exiting the chamber. To achieve this, a three-way PTFE Teflon valve was

used to switch flow between incoming and outgoing air which was then supplied to gas analyzers. Outgoing (chamber) air was analyzed for 25 minutes out of every half hour and incoming (house) air was analyzed for the remaining 5 minutes. A CO_2/H_2O analyzer (LICOR LI840A or LI7000) was used, along with a UV-absorption ozone monitor (Dasibi 1008-RS). CO_2 measurements were calibrated occasionally (roughly quarterly), and readings were not found to deviate significantly between calibrations. H_2O measurements were tested for biases and found to not deviate significantly during these experiments by comparing the H_2O analyzer output against calculated H_2O concentrations based on data from the relative humidity and temperature sensor (Vaisala HMP60) kept in the chamber; this sensor is considered more robust and reliable in the long term. Gas exchange parameters were calculated using procedures from Caemmerer and Farquhar (1981). Transpiration was calculated using equation 1,

$$E = \frac{u_e}{L} \cdot \frac{w_o - w_e}{1 - w_o \cdot 10^{-3}} \tag{1}$$

where E is transpiration in mmol m^{-2} s^{-1}, u_e is molar flow (mol s^{-1}) into the chamber, L is leaf area (m^2) in the chamber, w_e and w_o are the H_2O concentrations (ppth) entering and exiting the chamber respectively. Stomatal conductance was calculated using equation 2,

$$g_s = \frac{10^3 \cdot E\left(1 - \frac{w_o + w_e}{2 \cdot 10^3}\right)}{w_i - w_o} \tag{2}$$

where g_s is stomatal conductance in mmol m^{-2} s^{-1} and w_i is water vapor mole fraction (ppth) in the leaf's intercellular spaces. w_i was assumed to be at saturation at the leaf temperature (calculated at recorded leaf temperature via the Claussius Claperon equation). Thus, the reported conductance is a whole plant average assuming the measured leaf temperatures (see below) are representative for all leaves in the chamber.

CO_2 assimilation was calculated using equation 3,

$$A = \frac{u_e}{L}\left[c_e - \left(\frac{1 - w_e \cdot 10^{-3}}{1 - w_o \cdot 10^{-3}}\right) \cdot c_o\right] \quad (3)$$

where A is assimilation in μmol m^{-2} s^{-1}, c_e and c_o are the CO_2 concentrations (ppm) entering and exiting the chamber respectively. Isoprene emissions were calculated using equation 4,

$$I_e = \frac{u_e}{L}[i_o - i_e] \quad (4)$$

where I_e is isoprene flux from the leaf in nmol m^{-2} s^{-1}, i_e and i_o are concentrations (ppb) of isoprene entering and exiting the chamber respectively.

In addition to monitoring gas concentrations in the chamber, several other variables were monitored continuously. Air temperature and relative humidity were monitored in using a temperature/relative humidity sensor (Vaisala HMP60), which was suspended approximately 20 cm below the Plexiglas top of the chamber, above the cone of radiation from any of the LED lights. Three Teflon lined fine wire thermocouple temperature sensors (Omega Engineering Inc.) were used to monitor leaf temperatures at

three heights on the tree. These sensors have a small amount of thermal mass, and were applied such that they would remain in contact with the underside of a leaf being measured and thus out of direct radiation (shaded) from the LED lamps. Soil moisture was monitored using a dielectric moisture sensor (Decagon Devices) placed in the plant's pot. All the above sensor outputs were monitored at 10-second intervals and logged as one minute averages using a data logger (Campbell Scientific CR23X micrologger). For analysis purposes, the data recorded within one minute of the valve switching were removed. To minimize noise, and to ensure a steady state representation of chamber values, a mean of the last ten minutes of each 25-minute period was used. This ensured that the slight (1 L min^{-1}) change in flow through the chamber during the five-minute reference period was mixed out according to the measured turnover estimation within the chamber.

VOC samples were taken at regular intervals by passing a volume of air (200 mL) through a glass cartridge packed with a solid adsorbent (TENAX or Carbopack/Carbotrap stacked adsorbents). Samples of both house reference (incoming air) and chamber air were taken, which provided an assessment of background levels of the analyzed VOCs. Analysis of the samples was performed using a thermal desorber (ATD 400; Perkin Elmer, United Kingdom) coupled to an HP 5890-series II gas chromatograph equipped with a flame ionization detector (FID). Cartridges were heated to 220 °C and desorbed at 60 mL min^{1} into H_2 carrier gas. Samples were then cryo-focused on a low flow cold trap (PerkinElmer, UK) packed with Carbopack X (60/80) maintained at 5 °C. Secondary desorption occurred at 220 °C, and desorbed VOCs were

transferred through a heated capillary line held at 225 °C onto the analytical GC column for separation. Volatile compounds were separated on a 60 m × 0.25 mm MXT-624 Siltek®-treated stainless steel column (Restek Corporation, Bellefonte, PA, USA). The oven/column temperature was initially held at 35 °C for 3 min, then increased to 160 °C at a rate of 5 °C min^{-1}, and then to 220 °C at 20 °C min^{-1} heating rate and held at 220 °C for 14 min. The carrier gas (H_2) flow rate was set to 2 mL min^{-1}. Periodic system calibrations were carried out by diluting a multicomponent standard calibration mix (Scott-Marrin, Inc., CA) containing 10.35 ppm of isoprene (± 5% uncertainty) into humidified zero air (figure 1). For each analysis batch, several samples of the diluted standard gas were analyzed to assure calibration was within the expected range (Lahr et al., 2015).

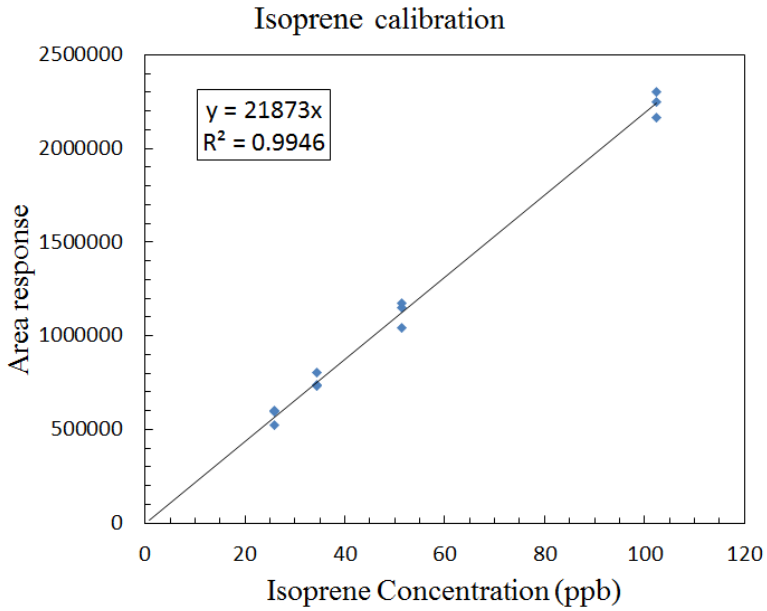

Figure 1. Example calibration curve for isoprene using a mass-flow controlled dilution of standard gas into zero air. Y-axis represents integrated area output from the GC, and the X-axis represents the calculated concentration of isoprene (ppb) in the sample analyzed.

During the ozone exposure experiments, OH radicals were formed in the chamber via the isoprene ozone reaction, with a standard temperature and pressure (STP) reaction rate constant of 12.8×10^{-18} cm^3 $molecule^{-1}$ s^{-1} and an OH yield of 0.26 (Malkin et al., 2010). OH would then have rapidly reacted with isoprene with a rate constant of 1.01×10^{-10} cm^3 $molecule^{-1}$ s^{-1} resulting in its removal (Atkinson 1994). A calculation was made to determine the amount of isoprene lost to this process. The maximum steady state OH concentration was calculated to be 8.07×10^4 molecules cm^{-3}, and the maximum amount of isoprene destroyed was on the order of 0.3 ppb. These calculations were made based on maximum measured chamber ozone and isoprene concentrations of 100 and 59 ppb respectively and a residence time of 10 minutes. 0.3 ppb isoprene represented less than 1% of chamber isoprene, and therefore this reaction chain was considered to not have significantly affected measured isoprene concentrations.

Leaf area of the seedlings was estimated after the trees were removed from the chamber using digital photography. Images of each leaf were taken next to a reference area for scale. The images were then processed using *Image-J* software, which provided a pixel count for the leaf as well as the reference area. These pixel counts were then converted to actual leaf areas based on the size of the reference area. Knowing the leaf area allowed for calculations of average fluxes (assimilation, transpiration, ozone fluxes, isoprene emission) per m^2 of leaf area in the chamber.

3.2. Experimental design

For this work, the above-described chamber was used to perform a series of experiments on isoprene emitting oak seedlings (*Quercus virginiana*, *Quercus alba* and

Quercus muehlenbergii). These species were chosen because they are known emitters of isoprene and were readily available at local plant nurseries at sizes that were reasonable for insertion into the chamber. Several characteristics of these trees were assessed, including how they were affected by stress in the form of drought and ozone exposure. First, for each experiment, a baseline was established after placing a plant into the chamber to determine rates of photosynthesis (A), transpiration, stomatal conductance (g_s), and isoprene emission (I_e) under 'normal' chamber conditions. These baseline measurements were used to test the statistical significance of the responses of the plants due to the changing chamber conditions. The effects on A, g_s, I_e, and ozone fluxes were tested for statistical significance using a student's t-test comparing them to baseline measurements ($\alpha = 0.01$). After inserting a specimen into the chamber, it took several weeks at times to acclimatize the seedling to the chamber's conditions. During this time, A, g_s, and I_e were generally increasing over time while the plant became adjusted to the light, temperature, and air composition conditions within the chamber. Not until after this acclimation period were baseline measurements taken; typically three weeks were needed for acclimation. Because of the comparatively long duration of this acclimatization period and the length of the experiments (ranging from 14 to 70 days), no same-species replicates of potted plant measurements were performed. Results from single experiments are often used in gas exchange studies (e.g. Holzinger et al., 2000 and Kesselmeier et al., 1998) because averaging results tends to obscure relationships that are clear when data from one trial is examined (Loreto and Sharkey, 1990).

Assessing the impact of drought on the plants was done simply by withholding water. Allowing the soil moisture to drop over time while monitoring photosynthesis, transpiration, isoprene emissions and ozone fluxes permitted an analysis of how these processes were affected by drought stress. Significant reductions in photosynthesis and transpiration were expected, but minor drought stress was not expected to impact isoprene emissions. A drought experiment was performed on a *Q. alba* specimen in which the plant was exposed to three drying cycles with periods of re-watering between cycles. This allowed for the effects of water stress to be analyzed, as well as the effects of repeated drought conditions on the plant's physiology.

To assess the impacts of ozone on these species, they were fumigated with several concentrations of ozone for extended periods of time. A diurnal cycle of ozone was used, with elevated concentrations during the day and reduced concentrations at night to emulate typical environmental conditions. Ozone experiments lasted between 14 and 21 days, with a daytime ozone range from 60 to 100 ppb incoming ozone. Because isoprene reacts with ozone in the gas phase, it was important to look for evidence that these reactions were occurring in the chamber. The gas phase reaction of ozone with isoprene proceeds slowly at STP ($k = 12.8 \times 10^{-18}$ cm^3 $molecule^{-1}$ s^{-1}), so there were likely only low levels of reaction products generated in the free air within the chamber (Atkinson, 1994). An estimate of 0.42 ppb MACR was made as the upper limit generated within the chamber based on the highest ozone (100 ppb) and isoprene (59 ppb) concentrations recorded in the chamber during all experiments, using a residence time of 10 minutes and a MACR yield of 0.37 (Aschmann and Atkinson 1994). This

was nearing the detection limit for MACR of 0.22 ppb based on the methods used in this work. If, however, ozone entered the stomata in high concentrations and was able to react with elevated levels of isoprene in the stomatal cavity, it would likely have been possible to detect significant concentrations of MACR and MVK. If concentrations of these products were detected at greater than predicted concentrations based on chamber isoprene and ozone concentrations, and indeed if they were detected at significant concentrations at all, it indicated ozone entering and reacting with isoprene in the intercellular spaces of the leaves, or possibly direct MACR emissions from the plant (Jardine et al., 2012; Jardine et al., 2013).

Another method for determining the amount of ozone entering the stomata was accounting for all other losses of ozone. Ozone was removed via the chamber surfaces and surface reactions on the stems and leaves of the seedlings in addition to the amount removed within the stomata. Assuming that the stomata are closed at night, all ozone removed at night was by plant and chamber surfaces. These reactions were expected to be 1st order with respect to ozone concentrations, so after measuring the surface reactions (nighttime flux) at several different ozone concentrations, a linear regression was used to estimate the surface removal at any ozone concentration. Subtracting the amount estimated by the regression from the total ozone removed while the lights were on (and stomatal conductance was larger than zero) yielded the amount removed via the stomata.

Wall losses of ozone within the chamber were measured for each ozone exposure experiment. These losses ranged from 4-10% of incoming ozone concentrations, and

were assessed by running ozone through an empty chamber including a dry snag from a dead seedling in its lower part to simulate losses to plant stems. Losses differed slightly based on the size of the plant because the chamber was expanded for some of the larger seedlings. The losses were then subtracted from the total ozone removed in all experiments to determine the amount removed by the live plant parts only.

To determine the level of circadian control over photosynthesis, stomatal conductance and isoprene emission, these variables were monitored under constant light for prolonged periods. Before leaving the lights on for an extended period, baseline isoprene measurements were taken to determine the normal 24-hour cycle of emissions. The lights were then left on for periods of 60 and 84 hours while regularly taking VOC samples. In between the prolonged continuous light experiments the plant was allowed to re-acclimatize to a normal 12 hours' light per day schedule.

4. RESULTS

4.1. *Quercus alba* drought stress

4.1.1. *Quercus alba* drought stress introduction

A White oak (*Quercus alba*) seedling was used to assess the impacts of water stress (drought) on its physiology and isoprene emissions. The seedling was installed in the chamber and allowed to acclimatize to its environment for several weeks prior to performing these experiments. After the tree was established in the chamber, baseline measurements were taken for approximately three weeks. During this period, the seedling was kept well-watered. Measurements of E, g_s, A, and I_e were recorded during this period and used as comparison to the seedling in a water stressed state. Because incoming CO_2 was not explicitly controlled, some effect on A from fluctuating concentrations of CO_2 was observed. To adjust for this, during the baseline period a linear regression of daytime (11am –3pm) assimilation with respect to incoming CO_2 concentrations was performed (not shown). The assimilation values were then normalized with respect to this regression at 400 ppm (approximately 2.5 μmol m^{-2} s^{-1}). This is lower than typical values observed in the field; to put this into context, values of 5 – 15 μmol m^{-2} s^{-1} were often recorded via a leaf-level analyzer (CIRAS) at standard conditions (1000 PAR, 30 °C, 400 ppm CO_2) with water oaks (*Quercus nigra*) near Houston throughout the summer (not shown).

4.1.2. *Quercus alba* drought stress results

Figure 2 shows the timeline of this experiment, including the baseline period as well as the three drying cycles. Daily cycles of g_s and A can be seen, with peak values

occurring at midday, and minimum values occurring at night when the chamber lights were off. During the baseline period (days 0-20), daytime g_s was relatively constant at around 27 mmol m^{-2} s^{-1}. These values of bulk g_s were expectedly lower than in the field; values as high as 300 mmol m^{-2} s^{-1} at standard conditions were often recorded via a leaf-level analyzer for water oaks near Houston throughout the summer (not shown). I_e were between 14 and 18 nmol m^{-2} s^{-1} during this baseline period. This is again slightly lower than values expected in the field; Geron et al. (2001) cited a range of 22 to 79 nmol m^{-2} s^{-1} under standard conditions for American tree species (since leaves on trees in the chamber are on average exposed to both lower light levels and temperatures than standard conditions, this is not surprising). Daytime values of normalized A were, of course, steady at around 2.5 μmol m^{-2} s^{-1} since this was the period used to normalize A values. After the baseline period, the seedling was exposed to three drought cycles (days 21-34, 38-50, and 53-67). Water was withheld until measured soil moisture dropped below 10% by volume. In between drying cycles, the seedling was watered for 3-4 days to allow the soil to become fully saturated and for the seedling to recover.

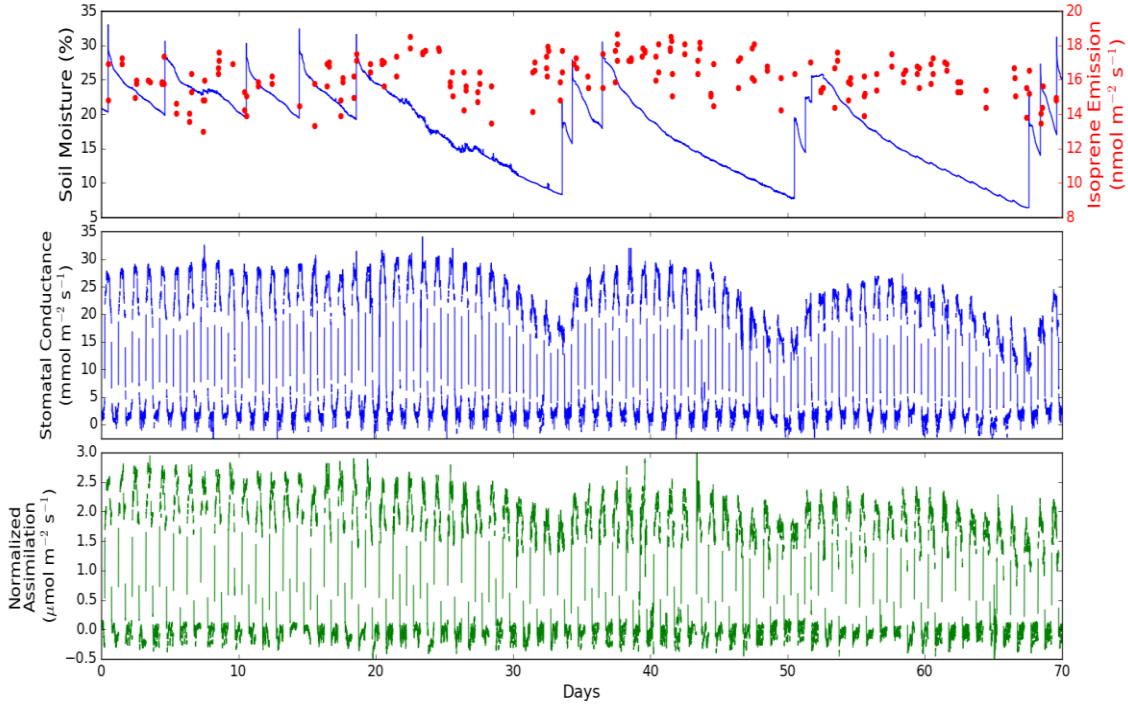

Figure 2. *Q. alba* drought timeline. Top panel shows soil moisture (%) as a blue line, and isoprene emission, I_e (nmol m^{-2} s^{-1}), as red dots. Middle panel shows stomatal conductance, g_s (mmol m^{-2} s^{-1}), as a blue line. Bottom panel shows normalized CO_2 assimilation, A (μmol m^{-2} s^{-1}), as a green line.

Stomatal conductance and assimilation declined along with soil moisture during the drying cycles. This decline did not begin until soil moisture went below 15%, as can be seen in figures 3 and 4. Stomatal conductance and assimilation remained relatively constant above 15% soil moisture, but declined steadily below that level of saturation. The threshold of 15% soil moisture represented the point at which the seedling began to experience water stress, but was well above the wilting point for this soil. In the first trial, g_s declined to 17.5 mmol m^{-2} s^{-1} (40% decrease; $p < 0.01$), and after the third trial it reached a minimum of 12 mmol m^{-2} s^{-1} (60% decrease from baseline; $p < 0.01$). Assimilation values declined to 1.6 μmol m^{-2} s^{-1} (36% decrease; $p < 0.01$) in the first

trial, and after the third trial declined to 1.25 μmol m^{-2} s^{-1} (50% decrease from baseline; $p < 0.01$). I_e remained relatively consistent and within the reference (baseline) range for this seedling throughout all three drought cycles, and thus did not show any significant changes ($p > 0.05$).

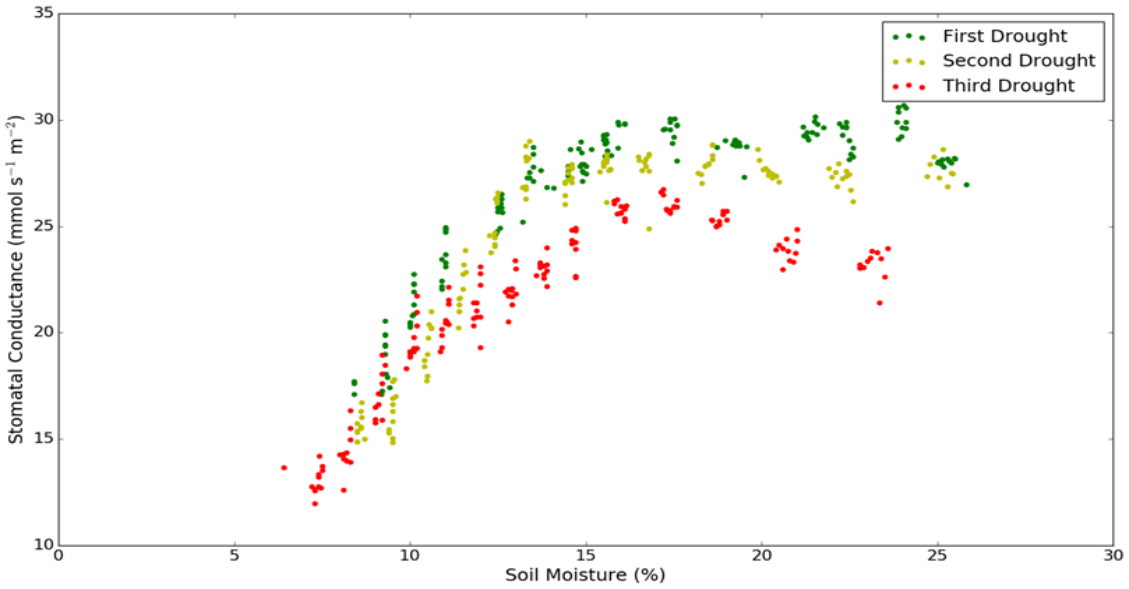

Figure 3. Relationship between stomatal conductance, g_s (mmol m^{-2} s^{-1}), and soil moisture (% by volume) for the three consecutive drought experiments. Data represent daytime (11 am – 3 pm) 10-minute means for each half hour during times of water stress (3-4 day recovery periods are excluded). Each successive trial (first, second, third) is displayed in its own color (green, yellow, and red respectively).

4.1.3. *Quercus alba* drought stress discussion

As expected, simulated drought on a *Q. alba* seedling had profound negative effects on its productivity. In response to water stress, the seedling closed its stomata to conserve its limited water resources. This resulted in significant declines in recorded transpiration (not shown), and thus g_s, illustrated in figure 3. As a result of smaller stomatal apertures, the seedling was unable to assimilate as much CO_2 compared to the

baseline period. This is evident in figure 4, which illustrates the positive relationship between A and soil moisture during these experiments. Along with these significant short term negative effects on g_s and A, the seedling showed a reduction in g_s and A after being re-watered. This hysteresis effect due to repetitive water stress was recorded, where g_s and A are reduced for each successive drought trial at a given level of soil moisture (figures 3 and 4). This is particularly evident when the seedling was not water stressed (above 15% soil moisture). This effect was likely because of damage to the plant due to repeated water stress which resulted in a reduction in the seedling's ability to open its stomata to pre-water stress levels.

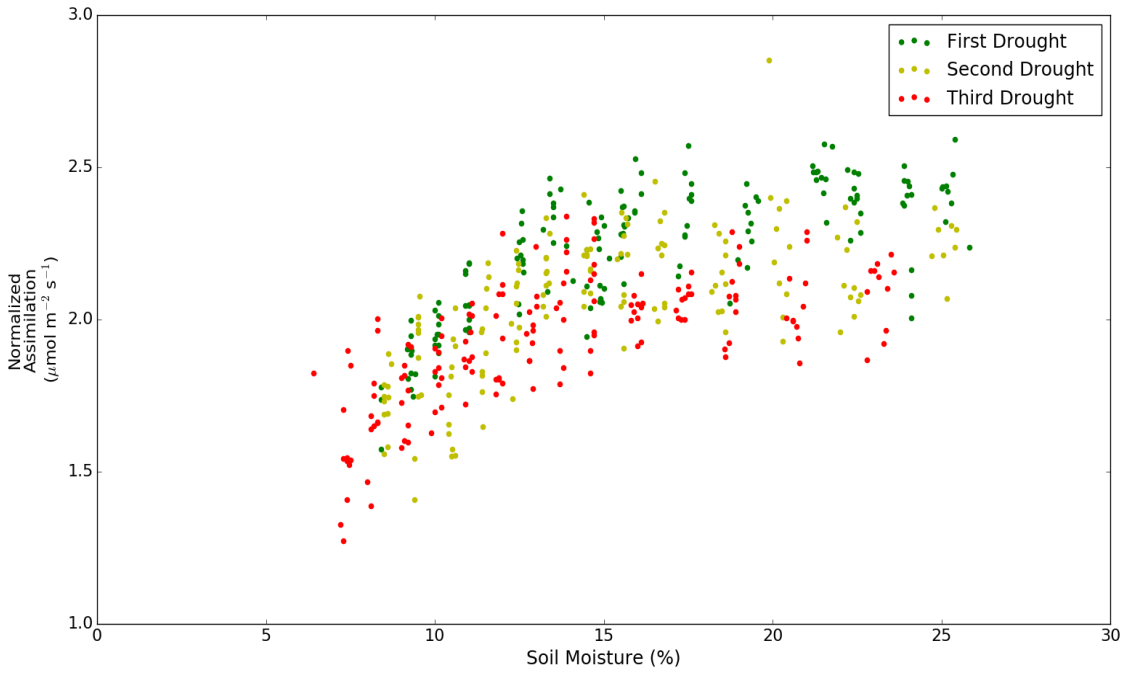

Figure 4. Relationship between normalized CO_2 assimilation, A (µmol m^{-2} s^{-1}), and soil moisture (% by volume) for the three consecutive drought experiments. Data represent daytime (11 am – 3 pm) 10-minute means for each half hour during times of water stress (3-4 day recovery periods are excluded). Each successive trial (first, second, third) is displayed in its own color (green, yellow, and red respectively).

As expected, I_e was not affected by the mild water stress the seedling was exposed to and remained within the baseline range of variability for this seedling (14 to 18 nmol m^{-2} s^{-1}), even with significant changes in g_s. This is in stark contrast to the effect of g_s on A, which showed significant dependence on g_s. I_e remaining relatively constant, along with declines in assimilation of up to 50% resulted in significant changes in the percentage of assimilated carbon emitted as isoprene. Non-water stressed percentages were as low as 2.25%, but as the seedling reduced its rate of assimilation, the percentage climbed to as high as 4.25% (figure 5). Carbon isotope labelling studies have shown that while isoprene is synthesized from primarily recently assimilated carbon, there appears to be an alternative pool of carbon for plants to use in isoprene synthesis (Loreto et al., 2004; Affek and Yakir, 2003; Karl et al., 2002). This study supports that hypothesis, by showing that I_e was not affected by significant (50%) declines in assimilation rates. This indicates that either the newly acquired pool of carbon is large enough to continue to supply the isoprene pathway under mild water stress, or there is an alternative pool that isoprene synthesis activity has access to.

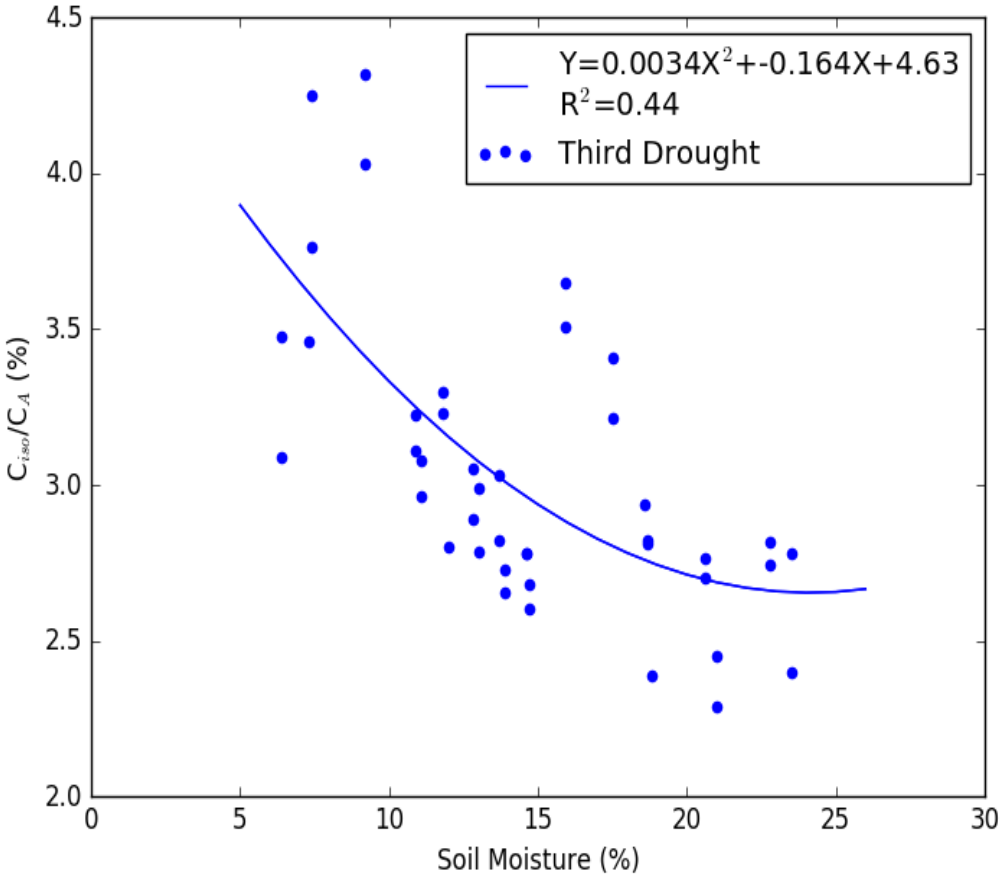

Figure 5. Relationship between the percentages of assimilated carbon emitted as isoprene (C_{iso}/C_A) and soil moisture (% by volume) during the third drought trial. Each point represents one isoprene sample and a ten-minute average of the assimilation and soil moisture at the time the sample was taken.

4.2. *Quercus alba* ozone exposure

4.2.1. *Quercus alba* ozone exposure introduction

To further examine the role that surface reactions play in ozone fluxes in canopies, specifically its partitioning between stomatal and non-stomatal sinks, a White oak (*Quercus alba)* seedling, the same specimen used in the above-mentioned drought experiment (section 4.1.), was fumigated with ozone. Due to an outbreak of aphids in

the laboratory, a mixture of olive oil, lavender oil, dish soap (*Dawn* brand) and water had been applied to the leaves via a spray bottle and allowed to dry on the leaves. This mixture was used because it was a recommended, pesticide-free treatment to eliminate the aphids. It turned out that this also provided an opportunity to further examine the role of surface reactions on ozone uptake. Lavender oil contains both mono- and sesquiterpenes in significant quantities, and because of the relatively low volatility of some of these isoprenoids, they remained on the leaf surfaces throughout the experiment (Munoz-Bermomeu et al., 2007). Due to one or more reactive double bonds in their structure, these compounds react readily with ozone, so they can effectively increase the rate of surface ozone fluxes. Similar to the previous experiment, the seedling was installed in the chamber and fumigated with ozone after allowing it to acclimatize to the chamber environment. For a plant without an isoprenoid coating, the expectation was that surface reactions would be responsible for comparatively small amounts of ozone removal, with the majority of ozone loss due to stomatal fluxes. Leaf surfaces are composed of recalcitrant substances that are resistant to oxidation via ozone exposure (Jetter et al., 2006). Meaning, leaf outer surfaces are designed to prevent damage due to oxidation, and therefore preserve plant structures.

Somewhat unexpectedly in this experiment, unusually high rates of surface ozone fluxes were observed (discussed below). At the time, it was not clear what caused this, but upon further investigation it became clear that adding the aphid treatment mixture to the leaves acted as a significant sink. Large fluxes at the leaf surface resulted in significant changes to the partitioning between stomatal and non-stomatal sinks and the

magnitude of the stomatal sink. On a leaf without this coating, ozone is not efficiently removed at the leaf surface, and therefore the ozone gradient at the stomatal opening remains large (assuming zero ozone within intercellular spaces, as is convention). Thus, the ozone gradient into the stomatal cavity allows for efficient 'pumping' of ozone into the leaf as CO_2 and H_2O enter and leave the intercellular spaces. I hypothesize that stomatal ozone quenching will have detrimental effects on plant productivity, and that the applied coating acted to reduce harm to the plant. This is because when ozone enters the stomata, it can oxidize membranes and intracellular structures within the leaf that are part of the photosystem. Because of such ozone-caused damage, the productivity of the plant will decline. If adding the mixture to the leaf surfaces reduced ozone concentrations significantly in the leaf boundary layer, the ozone gradient across the stomata will be reduced, and therefore reduce stomatal uptake of ozone. This mechanism is dependent on the resistance to transport in the leaf boundary layer; if resistance is high the surface sink will have time to remove ozone and 'protect' the stomata. If the resistance is low, as would be the case with a thin boundary layer, ozone concentrations would remain high at the leaf surface, despite the presence of a strong ozone surface sink. The depth of the boundary layer depends on the flow around the leaf; high flow results in a reduction in depth while low flow allows the leaf boundary layer to be maintained.

To test whether the coating played a significant role in ozone partitioning and if it had any effect on the productivity of the plant, similar ozone exposure regimes were performed to the same seedling one year apart. The first year ozone experiment was

done with the (dried) aphid treatment mixture on the leaves. The seedling was then allowed to senesce and grow new leaves the following spring, at which point the ozone exposure regime was repeated without the coating.

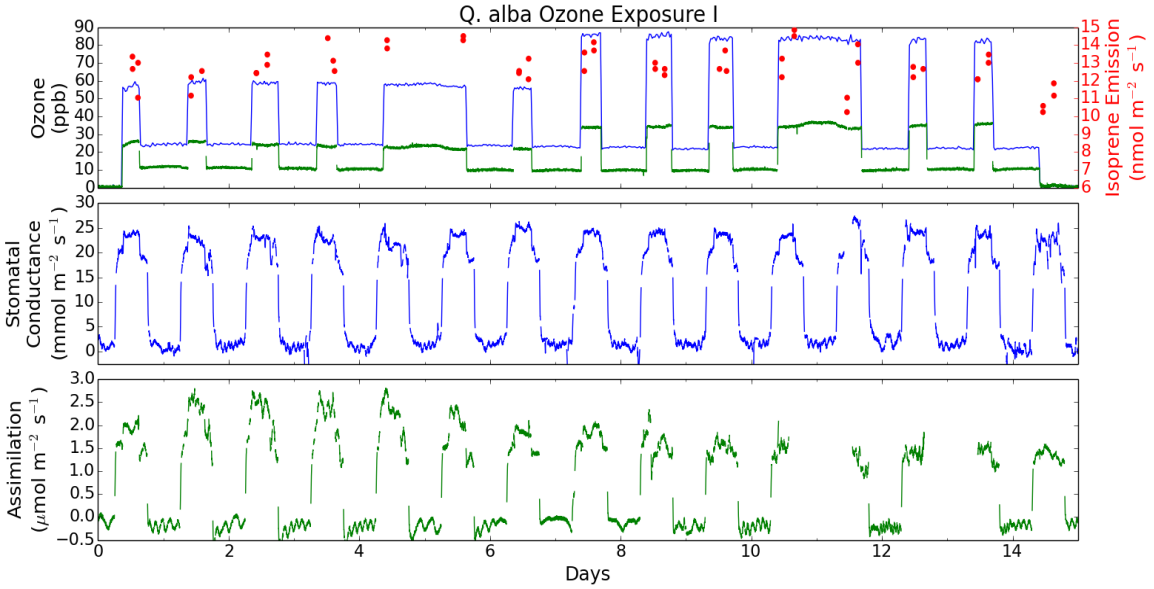

Figure 6. Timeline of first ozone experiment on *Q. alba* I. Top panel shows incoming ozone concentrations (ppb) as a blue line, chamber ozone concentrations (ppb) as a green line, and isoprene emissions, I_e (nmol m^{-2} s^{-1}), as red dots. Middle panel shows stomatal conductance, g_s (mmol m^{-2} s^{-1}), as a blue line. Bottom panel shows normalized CO_2 assimilation, A (μmol m^{-2} s^{-1}), as a green line.

During the first experiment, when the leaves were coated with the isoprenoid mixture, the *Q. alba* seedling was exposed to a diurnal cycle as can be seen in figure 6. This particular seedling had a one-sided leaf area of 0.178 m^2. Daytime ozone was added at 60 and 90 ppb for one week each respectively, while nighttime ozone was set to approximately 25 ppb. Nighttime ozone was left at elevated (daytime) concentrations for two nights (nights 4-5 and 10-11) to better estimate the rate of ozone removal to leaf surfaces.

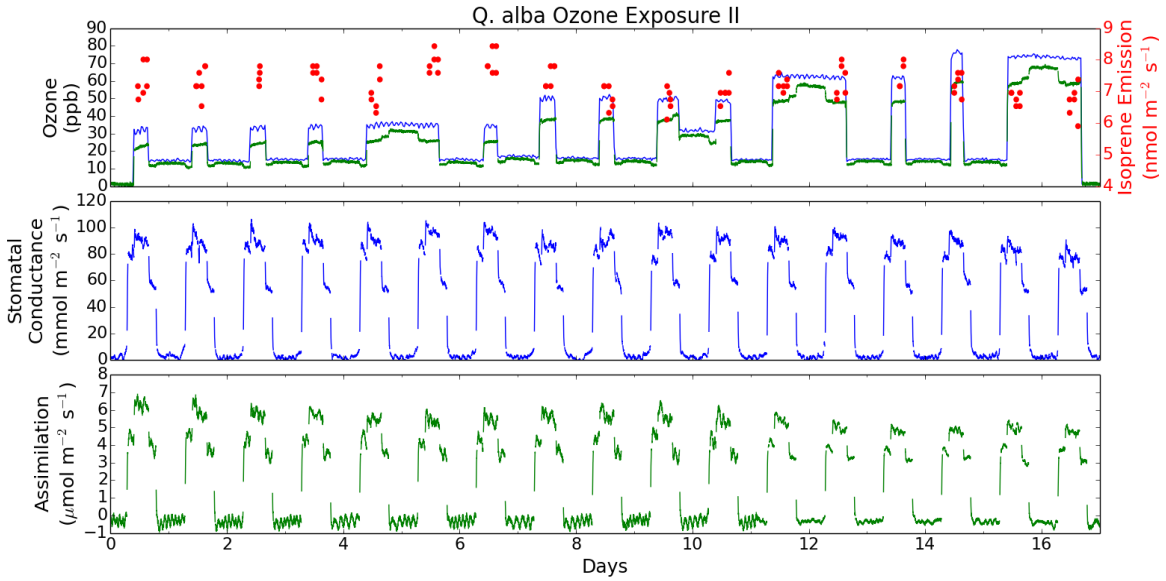

Figure 7. Timeline of second ozone experiment on *Q. alba* II. Top panel shows incoming ozone concentrations (ppb) as a blue line, chamber ozone concentrations (ppb) as a green line, and isoprene emissions, I_e (nmol m^{-2} s^{-1}), as red dots. Middle panel shows stomatal conductance, g_s (mmol m^{-2} s^{-1}), as blue line. Bottom panel shows normalized CO_2 assimilation, A (μmol m^{-2} s^{-1}), as a green line.

During the second experiment, when there was no coating on the leaves, the seedling was exposed to a similar diurnal cycle of ozone. This seedling had a one-sided leaf area of 0.0977 m^2. Daytime ozone was added at 35, 50, 60, 75 ppb for 7, 4, 3, and 3 days respectively. Nighttime ozone was left at elevated (daytime) concentrations for three nights (nights 4-5, 11-12, and 15-16) to better estimate the rate of surface ozone removal to leaf surfaces.

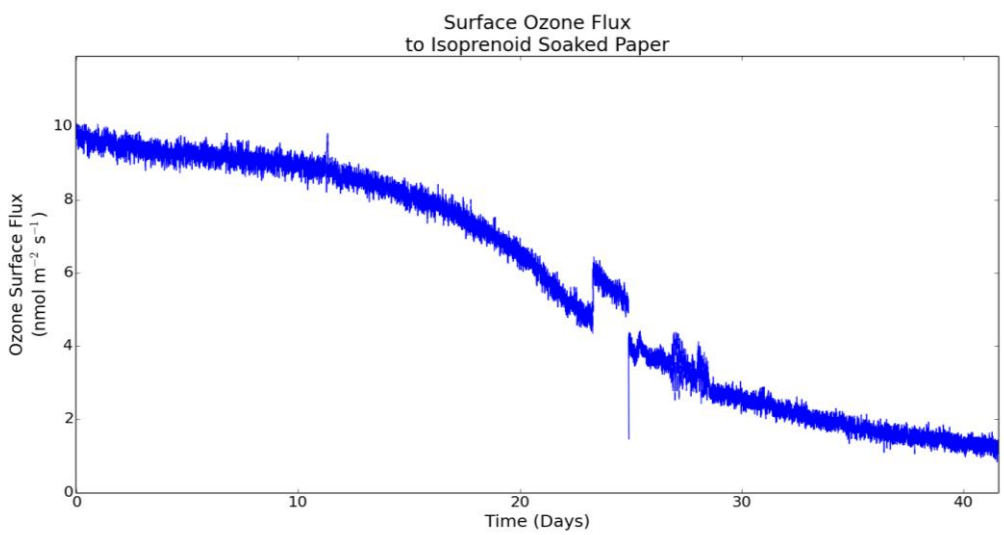

Figure 8. Ozone surface flux (nmol m^{-2} s^{-1}) for an isoprenoid-soaked piece of letter-size paper (8.5 by 11.0 inches; 0.06032 m^2 one-sided area).

After both above-mentioned experiments were completed, the isoprenoid mixture was applied to a piece of paper and installed in the chamber. The paper was sprayed with the mixture and allowed to dry overnight, and then suspended in the chamber by a fine wire thermocouple already in use in the chamber. The coated paper was then fumigated with approximately 65 ppb of ozone to verify that the coating was indeed acting as a significant sink for ozone. Prior to this, an untreated paper was tested, which showed minimal ozone removal. The coated paper removed as much as 56% of the incoming ozone when first installed in the chamber. This showed that the applied mixture was indeed a significant ozone sink, and that it was likely the cause for such unexpected surface fluxes on the treated plants. The fraction of ozone removed reduced over time, likely as its antioxidant capacity was diminished by ozone. The ozone flux was 9.8 nmol m^{-2} s^{-1} when first installed in the chamber, and diminished to as low as 1.2 nmol m^{-2} s^{-1} after being fumigated for 42 days (figure 8). A linear regression was

performed on the surface ozone fluxes to the paper to determine the rate of change of this flux. Because the rate of change was non-linear, two separate rates were estimated: one for the first 10 days, and another for days 10-30. For the first 10 days, the surface flux reduced by 0.085 nmol m^{-2} s^{-1} day^{-1}, and for days 10-30 the surface ozone flux reduced by 0.322 nmol m^{-2} s^{-1} day^{-1}. Because of the short duration of the ozone exposure experiments (e.g. 14 days for *Q. alba* I), and the fact that ozone was decreased at night during these experiments, accumulated ozone did not reach above 12000 ppb•hours in any of the ozone exposure experiments. For this reason, the slope derived from the first 10 days of the paper experiment was used. A rate of -1.614×10^{-3} % $(ppb•hour)^{-1}$ was found for the first 10 days. This rate was compared to data from later *Q. alba* and *Q. virginiana* (see sections 4.3. and 4.4.) experiments to determine if the rate of change of the coating's sink could explain results from those experiments.

4.2.2. *Quercus alba* ozone exposure results

During the first experiment, the seedling displayed no evident initial changes in g_s and I_e, however, A declined from approximately 2.5 μmol m^{-2} s^{-1} to 1.5 μmol m^{-2} s^{-1} (40% reduction; $p < 0.01$) by the end of the experiment. Possible explanations for this decline are given in the discussion section below. I_e remained within the baseline range of variability for this seedling during this experiment.

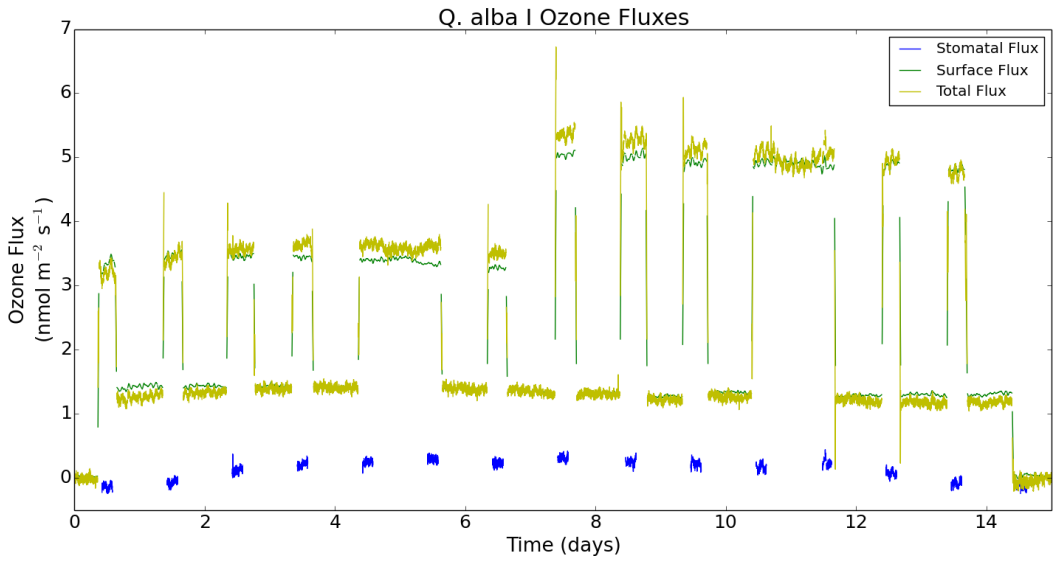

Figure 9. Plant ozone fluxes (nmol m^{-2} s^{-1}) during the *Q. alba* I ozone experiment. Total plant fluxes are represented by a yellow line, plant surface fluxes are represented by a green line, and stomatal fluxes are represented by a blue line.

Ozone fluxes to the plant during *Q. alba* I ranged from 3.2 to 5.4 nmol m^{-2} s^{-1} with the majority apportioned to surface fluxes. Surface fluxes ranged from 3.1 to 5.1 nmol m^{-2} s^{-1}, while stomatal fluxes ranged from negative (non-physical) to 0.3 nmol m^{-2} s^{-1} (figure 9). Surface fluxes represented between 93 and 100% of the total plant flux, while stomatal fluxes represented between 0 and 7%. The small difference between daytime and nighttime total plant uptake on the night with elevated ozone (figure 6, nights 4-5 and 10-11) shows the very small relative contribution of the stomatal fraction for this experiment, and the dominance of the surface sink. This is evident in the near-zero ozone deposition velocities for stomata as well (figure 10), but note that deposition velocities maximized around day 5 into the experiment, before ozone concentrations were increased.

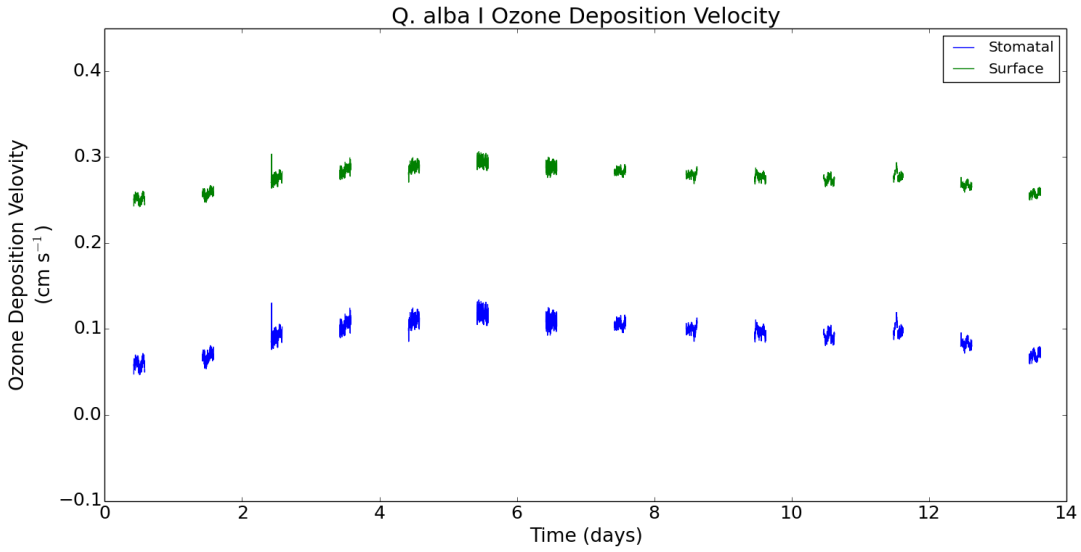

Figure 10. Ozone deposition velocities (cm s^{-1}) for the *Q. alba* I ozone experiment. Stomatal deposition velocities are represented by a blue line, and surface deposition velocities are represented by a green line. Data represent daytime (11 am – 3 pm) values only.

During the second experiment, the seedling displayed no evident initial changes in I_e, however, A declined from approximately 6.8 μmol m^{-2} s^{-1} to 5.1 μmol m^{-2} s^{-1} (25% reduction; $p < 0.01$) by the end of the experiment and g_s declined from 95 to 90 mmol m^{-2} s^{-1} (5% reduction; $p < 0.01$). Possible explanations for these declines are given in the discussion section below. I_e remained within the normal range of variability for this seedling during this experiment (6 to 8.5 nmol m^{-2} s^{-1}; $p > 0.05$).

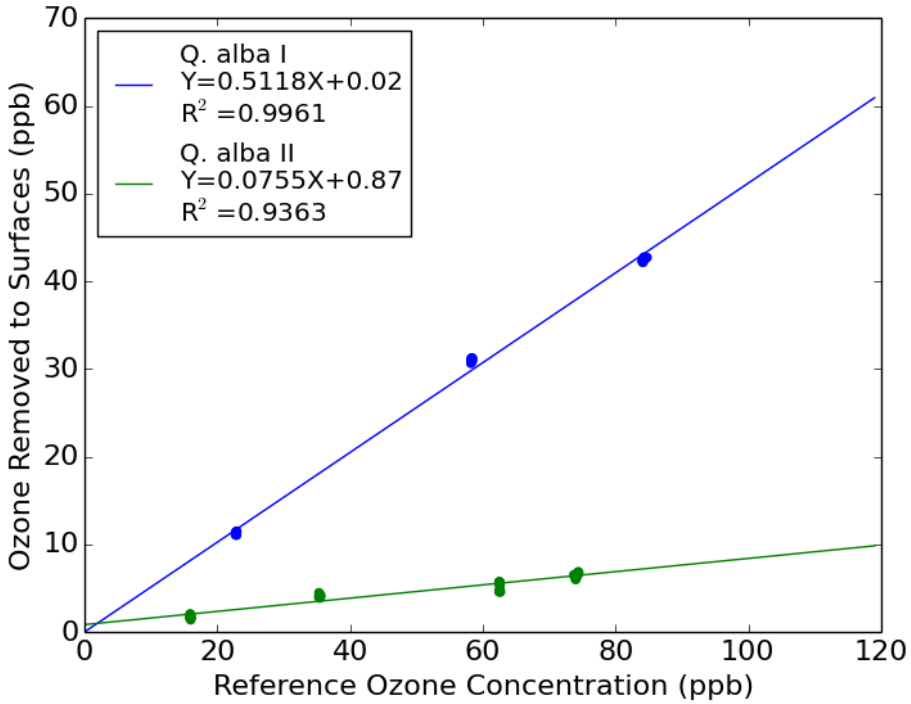

Figure 11. Relationship between incoming ozone reference (ppb), and amount of ozone removed to plant surfaces (Δ ppb) for both *Quercus alba* ozone experiments. Data represent nighttime (10 pm – 4 am) 10-minute means for each half hour. Blue points and line represent *Q. alba* I with terpenoid coating on leaves, green points and line represent *Q. alba* II without the coating.

During the second portion of this experiment, where the leaves were not terpenoid coated, dramatically different relative ozone fluxes were recorded. The partitioning of stomatal compared to non-stomatal fluxes were more similar to experiments with other species (e.g. *Quercus muehlenbergii* ozone exposure, section 4.4.) Total plant ozone fluxes during the *Q. alba* II experiment ranged from 1.5 to 2.7 nmol m^{-2} s^{-1}, but unlike *Q. alba* I, were dominated by stomatal fluxes. Surface fluxes ranged from 0.3 to 0.9 nmol m^{-2} s^{-1}, while stomatal fluxes were between 1.0 and 1.7 nmol m^{-2} s^{-1} (figure 12). The ozone deposition velocities (both to surfaces and stomata)

between the two experiments were significantly ($p < 0.01$) different because of the higher stomatal and lower surface fluxes in *Q. alba* II. During this experiment, surface fluxes represented between 20 and 46% of the total plant flux, while stomatal fluxes represented between 53 and 79%. The range in these fractions was due to stomatal fluxes changing over time while surface fluxes remained near constant at a given concentration. When ozone was initially turned on, stomatal uptake was high, but as exposure accumulated, stomatal fluxes steadily decreased. This was the case at all concentrations, however it was most notable when ozone was at its highest (days 14-16). A discussion of this process as well as possible consequences for the plant's productivity are given below.

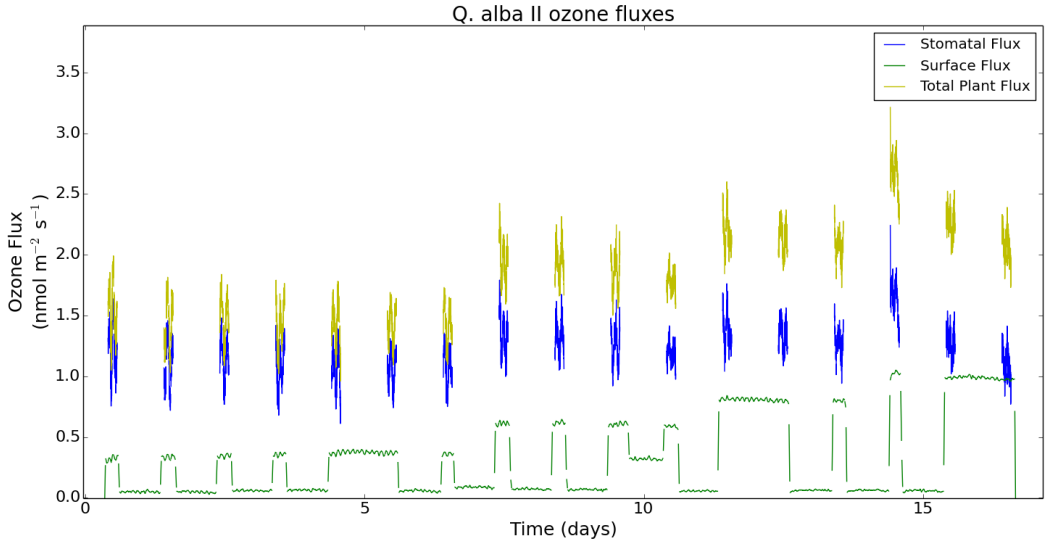

Figure 12. Plant ozone fluxes (nmol m^{-2} s^{-1}) during the *Q. alba* II ozone experiment. Total plant fluxes are represented by a yellow line, plant surface fluxes are represented by a green line, and stomatal fluxes are represented by a blue line.

Unlike in *Q. alba* I, during *Q. alba* II, the seedling displayed declines in g_s. In addition to a decline in g_s, the magnitudes of g_s and A were not similar between the two trials. This occurred because *Q. alba* II was unintendedly run at a lower temperature compared to *Q. alba* I (mean daytime leaf temperatures of 31 and 26 °C for *Q. alba* I and II respectively, not shown). This resulted in greater g_s and A during *Q. alba* II, and lower I_e. I discuss whether this was a main driver in the difference in ozone partitioning below.

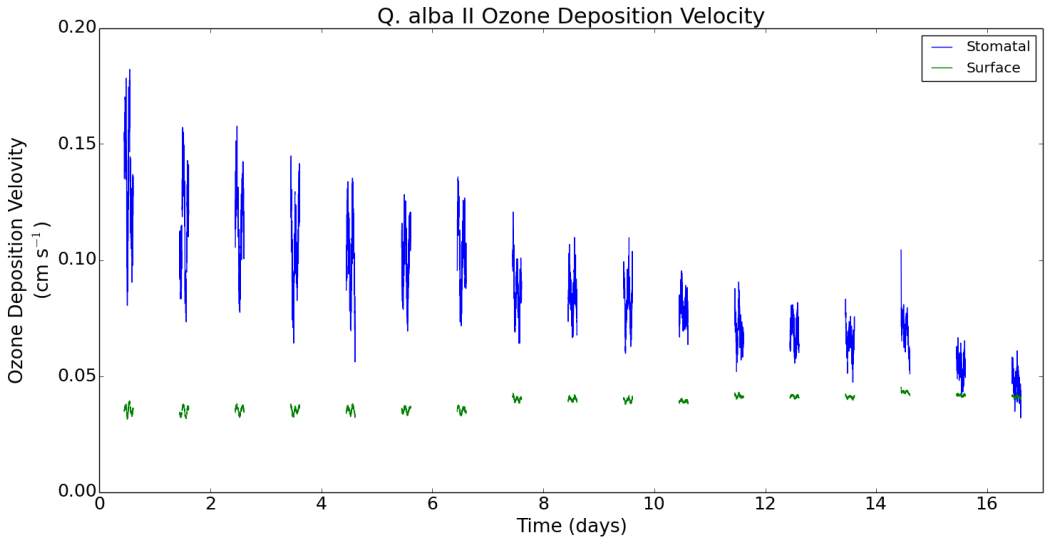

Figure 13. Ozone deposition velocities (cm s^{-1}) for the *Q. alba* II ozone experiment. Stomatal deposition velocities are represented by a blue line, and surface deposition velocities are represented by a green line. Data represent daytime (11 am – 3 pm) values only.

4.2.3. *Quercus alba* ozone exposure discussion

I think that the addition of a terpenoid coating in this experiment was the main driver in partitioning ozone losses between stomatal and non-stomatal pathways. The coating provided a strong sink for ozone in the chamber, and it was enough to dominate all other sinks. It overshadowed the magnitude of the stomatal sink, and it appeared to

reduce the magnitude of the stomatal sink as well. Jud et al. (2016) showed that a strong surface ozone sink can reduce stomatal ozone fluxes by reducing ozone in the leaf boundary layer. This was likely the mechanism in place in these experiments, causing a lower stomatal uptake on coated leaves (compares Figures 9 vs. 12). If ozone concentrations in the leaf boundary layer were efficiently reduced on coated leaves, this would have resulted in reduced ozone concentrations near the stomata. This in turn would have reduced the stomatal ozone gradient, and caused reduced diffusion into the stomatal cavity. For untreated leaves, the magnitude of the stomatal sink was strongly reduced over time (figures 12 and 13, days 14-16); this indicated that the effective removal within the stomatal cavity was decreasing over time, and this was likely due to oxidation of the surfaces responsible for the ozone reaction. The effect is more evident in the deposition velocities for the two experiments (figures 10 and 13; $p < 0.01$); on untreated leaves, the deposition velocity to the stomata clearly decreased over time, while deposition velocities to treated leaves were maintained at first, then declined slightly. Additionally, the *Q. alba* II experiment resulted in significant stomatal ozone fluxes, however neither MACR nor MVK were detected in these experiments. For these reasons, I have to conclude that the major ozone sink within the stomata was to intercellular surfaces, and not to gas-phase reactions with isoprene in the stomatal cavity.

A ‘protective role’ offered by the coating was likely as it appeared to reduce stomatal fluxes. This role was not indicated in the productivity of the treated vs untreated experiments however; both showed declines in A, and *Q. alba* I (coated leaves) had greater relative declines (40%) in A. Reductions in A in both experiments

indicated that the stomatal flux that was measured was going to surfaces within the stomatal cavity that were part of the plant's photosystem. Because significant reductions in productivity were noted in both experiments, a 'protective role' offered by this coating needs further study to determine its effectiveness. Neither experiment affected g_s to a significant degree; this shows that even without the 'protective' coating, the stomata were not significantly affected in their ability to open and close over time during these experiments.

An inconsistency with this experiment was that the two experiments were run at different temperatures, causing different magnitudes of g_s, A, and I_e. Further study is needed to determine how significant a role this played in ozone partitioning. It is possible that higher rates of stomatal ozone uptake recorded during *Q. alba* II were enhanced compared to *Q. alba* I because of the larger g_s during that experiment. It is unlikely, however, that the magnitude of the surface sink was altered because of this discrepancy. This is because the lamps were off at night during both experiments, and assessments of surface reactions were all measured at night by design. For both experiments, the average nighttime (10 pm to 4 am) temperature was within one degree Celsius: 23.4° C and 24.1° C for *Q. alba* I and II respectively. Additional evidence that the dissimilar g_s during both experiments did not strongly affect the stomatal ozone uptake exists in a later experiment, where a *Q. alba* (the same specimen) was exposed to ozone while restricting water (see *Quercus alba* drought + ozone exposure, section 4.3.). The water stress placed on the plant caused it to close its stomata, allowing measurements of stomatal ozone uptake at a range of g_s. There appears to be a threshold

of g_s above which stomatal ozone uptake was not affected. Below this threshold, stomatal ozone uptake declined with g_s, however above this threshold it remained constant. Figure 19 shows this relationship, displaying a g_s threshold of approximately 15 mmol m^{-2} s^{-1}. Further discussion of that experiment is made in section 4.3. below. Since both experiments were performed with well-watered specimens, they both had g_s above this threshold. Because of this, I conclude that the large deviation in g_s for the two experiments likely had a minor effect on stomatal ozone uptake.

4.3. *Quercus alba* drought + ozone exposure

4.3.1. *Quercus alba* drought + ozone exposure introduction

For this experiment, a White oak (*Quercus alba)* seedling was exposed to ozone while allowing it to become water stressed. This experiment was performed to assess the impact of drought on ozone uptake, and any cumulative effect these two stressors have together. This seedling had a one-sided leaf area of 0.178 m^2, and was the same specimen used in the above-mentioned ozone and drought experiments (sections 4.1. and 4.2.). As discussed above, this seedling had an isoprenoid coating applied to its leaves, which had significant effects on ozone uptake partitioning. Although the partitioning of ozone sinks was not what one would expect for an untreated specimen, it was possible to draw conclusions about the relationship between stomatal conductance and stomatal ozone fluxes. It was likely that a small portion of the isoprenoid coating had been oxidized by the time this experiment took place. Similar to the paper experiment, the coating diminished over time, and because the tree had been in the chamber under a two-week ozone experiment prior to this experiment, a portion of the coating had likely been

oxidized already. However, based on the rate of decline of surface ozone fluxes as a function of ozone concentration-hours in the paper experiment (-1.614×10^{-3} % $(ppb \bullet hour)^{-1}$), only approximately 0.02% of the surface flux from the applied coating was oxidized by the start of this experiment. This is consistent with the measurements taken in this experiment, as indicated by dominant surface fluxes to the lingering isoprenoid coating. The small difference between day and night chamber ozone concentrations on nights 7-8 and 18-19 (figure 14) and the high surface fluxes of ozone in this experiment were similar to those of coated leaves described in *Q. alba* I above (see section 4.2.).

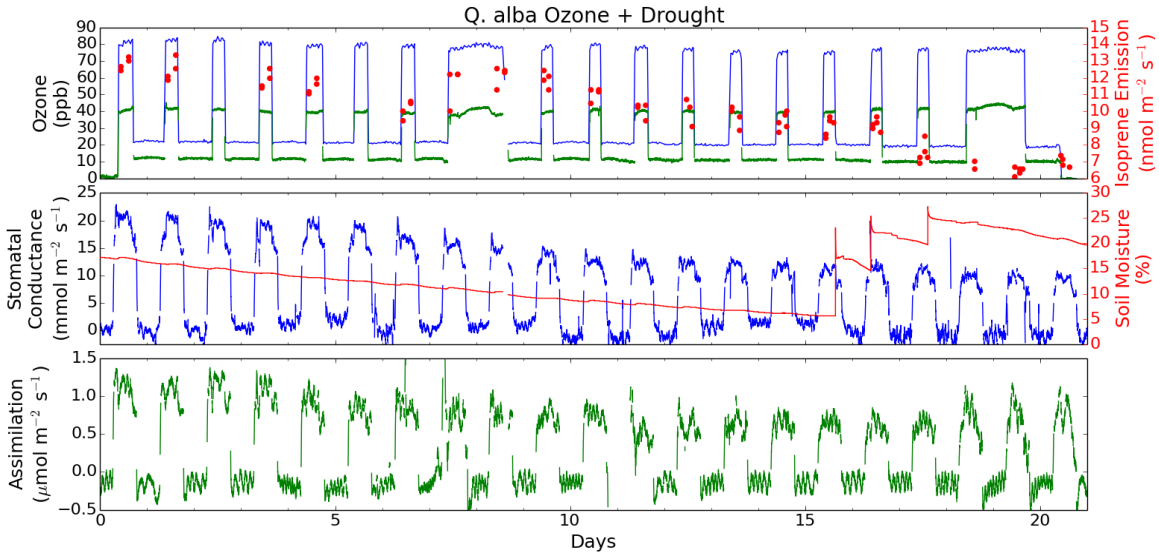

Figure 14. Timeline of drought + ozone exposure experiment on *Q. alba*. Top panel shows incoming ozone (ppb) as a blue line, chamber ozone concentrations (ppb) as a green line, and isoprene emissions, I_e (nmol m^{-2} s^{-1}), as red dots. Middle panel shows stomatal conductance, g_s (mmol m^{-2} s^{-1}), as a blue line, and soil moisture (%) as a red line. Bottom panel shows CO_2 assimilation, A (μmol m^{-2} s^{-1}), as a green line.

After installing the seedling in the chamber and allowing it to become acclimatized for several weeks, water was withheld until the soil moisture reached 5.5% by volume. The seedling was fumigated with a diurnal cycle of ozone, as described above (section 4.2.1), with daytime concentrations of 80 ppb and nighttime concentrations of 20 ppb. As the previous *Quercus alba* ozone experiments were performed under well-watered conditions, this experiment permitted an examination of the effects of ozone fumigation at a range of g_s values. It also allowed an assessment of how these two stressors affected the seedling when combined.

As a result of the water stress, the plant's stomata should begin to close, and this should affect the rate of stomatal ozone uptake. Smaller stomatal apertures will restrict the flow of gases into the intercellular spaces, resulting in reduced assimilation and ozone uptake. Figure 14 shows the timeline of this experiment, including the steady decline of soil moisture as the 'drought' progressed. Beginning on day 15, the seedling was re-watered and monitored for any signs of recovering from the water stress.

4.3.2. *Quercus alba* drought + ozone exposure results

As expected, drought and ozone exposure had significant negative effects on the physiology of this seedling. Reductions in g_s, A, and I_e were recorded during this experiment. g_s was initially 22 mmol m^{-2} s^{-1}, and declined to as low as 10 mmol m^{-2} s^{-1} by the end of the experiment (54% reduction; $p < 0.01$). The past drought experiment (see section 4.2.1 above) with this exact specimen yielded g_s as low as 12 mmol m^{-2} s^{-1} at the end of its third drought cycle. In this drought + ozone experiment, g_s declined until re-watering began on day 15 (see figure 14), and remained steady after this point.

No significant ($p > 0.05$) recovery in g_s was recorded from this seedling after re-watering as during the prior drought experiments, however significant recovery of A was recorded ($p < 0.01$).

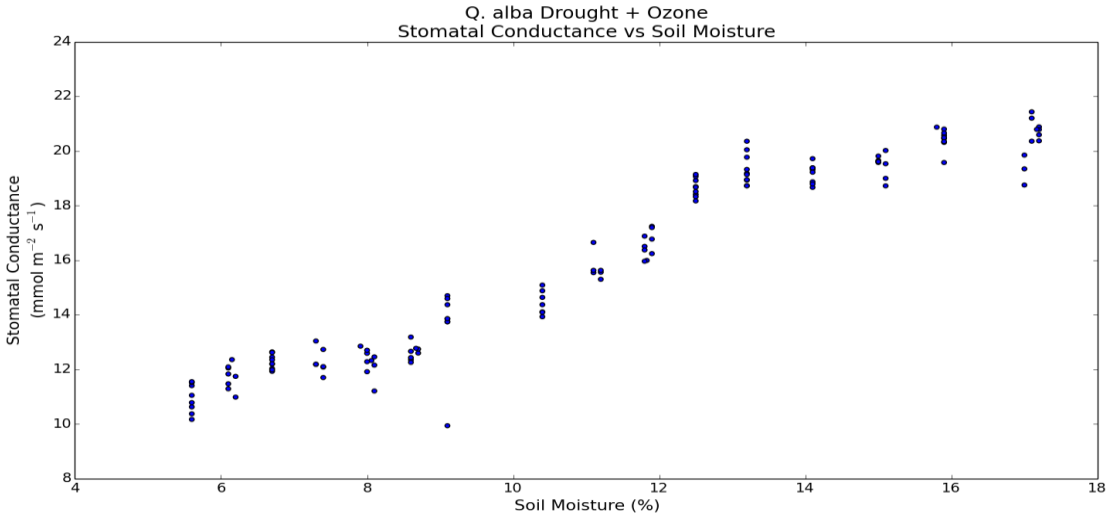

Figure 15. Relationship between stomatal conductance, g_s (mmol m^{-2} s^{-1}), and soil moisture (% by volume) for the drought + ozone exposure experiment. Data represent daytime (11 am – 3 pm) 10-minute means for each half hour during times of water stress (data from post re-watering excluded).

Figure 15 shows the relationship observed between g_s and soil moisture. Simultaneously, A declined from 1.3 µmol m^{-2} s^{-1} at the onset of the experiment, to as low as 0.6 µmol m^{-2} s^{-1} by the end of the experiment (53% decline; $p < 0.01$). Similar to the past drought experiments with this specimen, a significant positive relationship was observed at soil moistures below 15%, with near constant A above this threshold (figure 16).

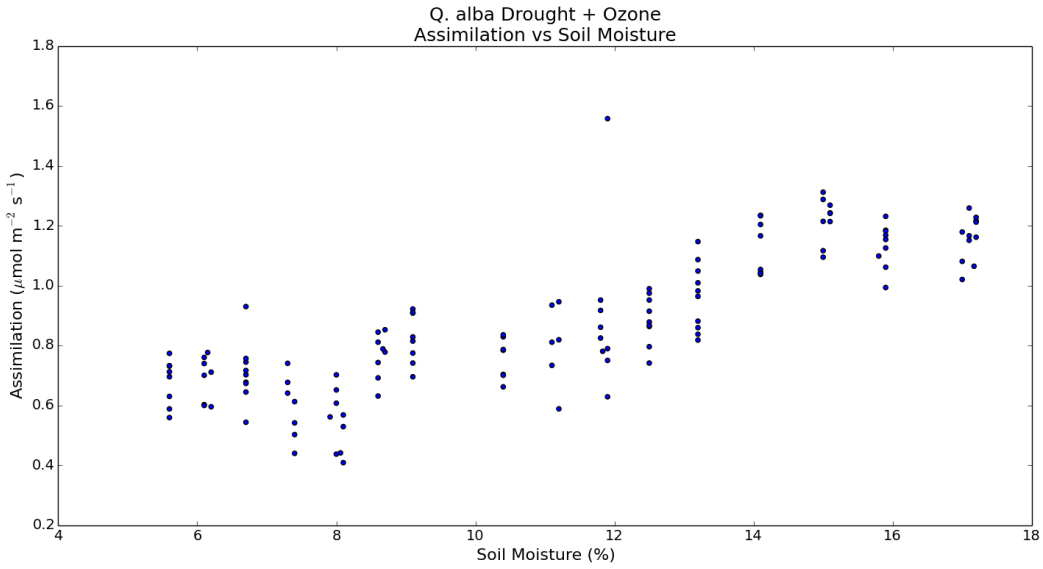

Figure 16. Relationship between CO_2 assimilation, A (μmol m^{-2} s^{-1}), and soil moisture (% by volume) for the drought + ozone exposure experiment. Data represent daytime (11 am – 3 pm) 10-minute means for each half hour during times of water stress (data from post re-watering excluded).

Unlike the past drought experiments with this specimen, significant declines in I_e were observed. I_e was initially 13.5 nmol m^{-2} s^{-1}, and declined to as low as 6.0 nmol m^{-2} s^{-1} by the end of the experiment (55% decline; $p < 0.01$). This was in stark contrast to the past drought experiment with this specimen, during which no significant changes in I_e were observed throughout three consecutive drought cycles. The reductions observed here were thus more likely due to induced senescence caused by the combination of ozone and water stress as discussed below.

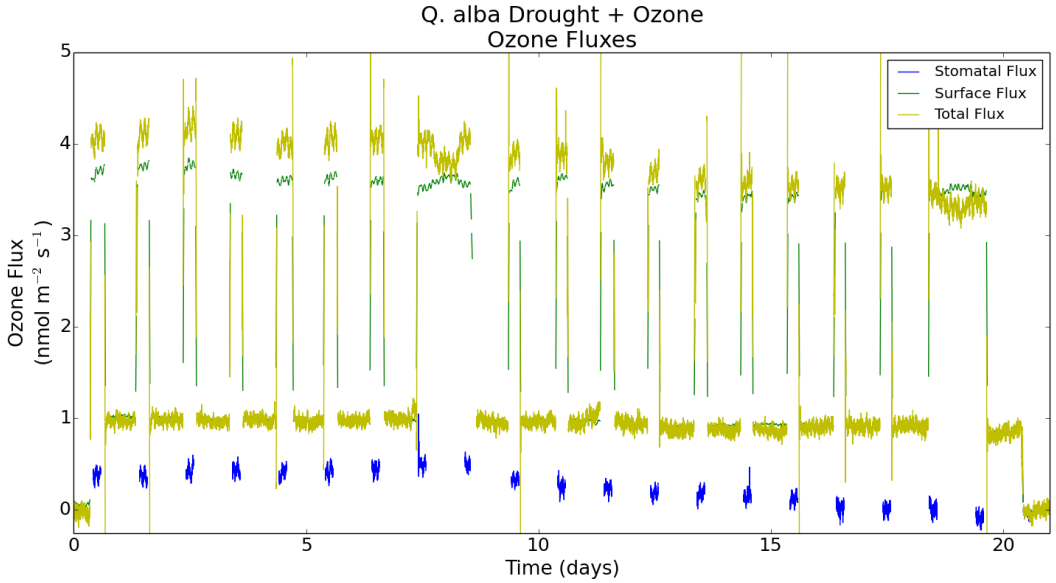

Figure 17. Plant ozone fluxes (nmol m^{-2} s^{-1}) during the *Q. alba* drought + ozone experiment. Total plant fluxes are represented by a yellow line, plant surface fluxes are represented by a green line, and stomatal fluxes are represented by a blue line

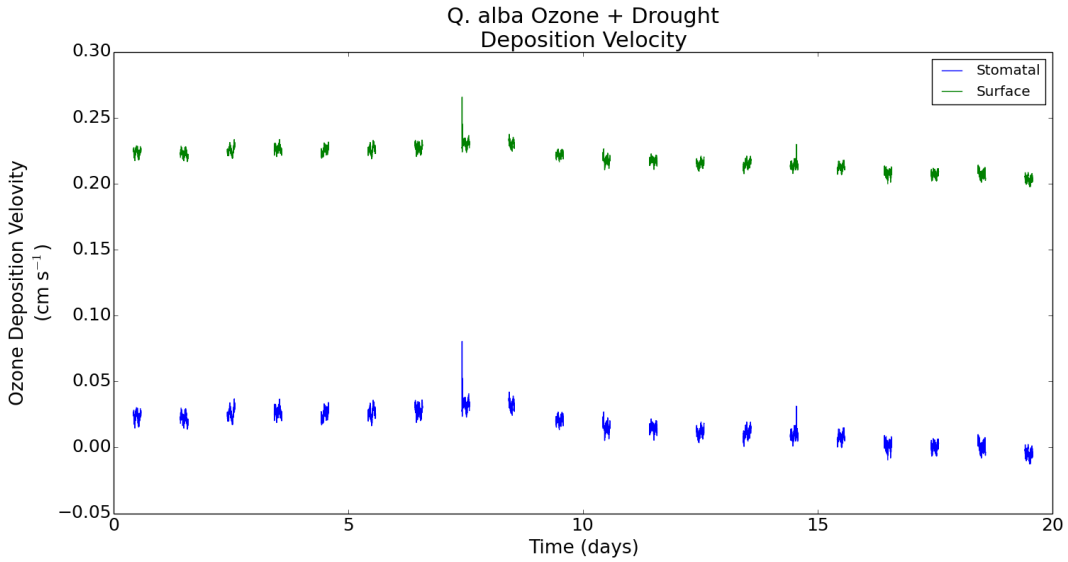

Figure 18. Ozone deposition velocities (cm s^{-1}) for the *Q. alba* drought + ozone experiment. Stomatal deposition velocities are represented by a blue line, and surface deposition velocities are represented by a green line. Data represent daytime (11 am – 3 pm) values only.

4.3.3. *Quercus alba* drought + ozone exposure discussion

Combining drought and ozone fumigation was designed to examine the relationship between stomatal conductance and ozone uptake as well as any physiological effects of these two stressors in combination. This was somewhat compromised by the addition of the isoprenoid coating. Past research has shown that combined drought and ozone exposure can lead to induced senescence and reduced photosynthesis (Hayes et al., 2015). The results of this experiment supports these findings, as significant declines in A, g_s, and I_e along with visible yellowing of the foliage were observed (figure 20). No visible damage had been observed in the previous *Q. alba* drought experiments. Therefore, I think that the senescence observed in this experiment was due to an additive effect of drought with ozone exposure.

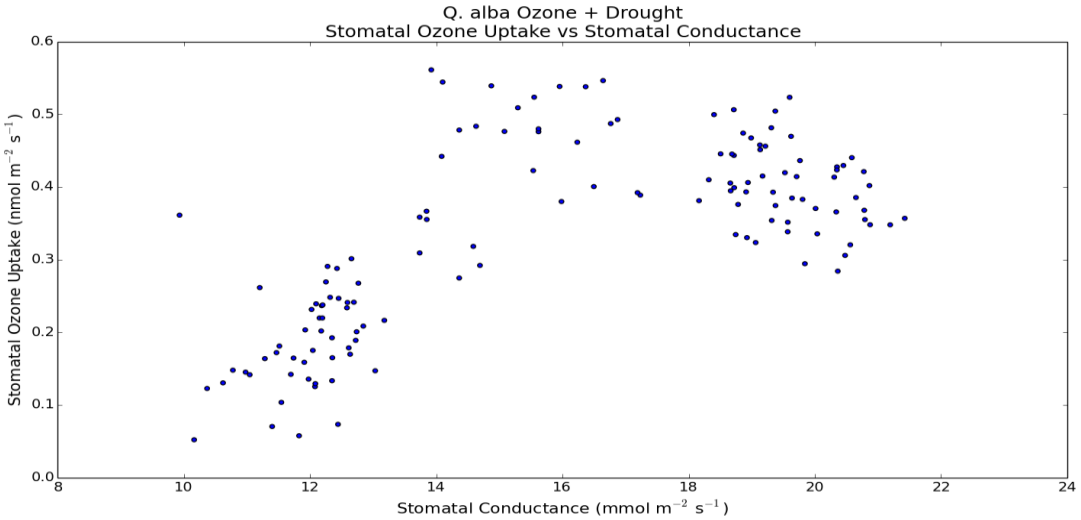

Figure 19. Relationship between stomatal conductance, g_s (mmol m^{-2} s^{-1}), and stomatal uptake of ozone (nmol m^{-2} s^{-1}) for the drought + ozone exposure experiment. Data represent daytime (11 am – 3 pm) 10-minute means for each half hour during times of water stress (data from post re-watering excluded).

As the plant became increasingly water stressed, it responded by closing its stomata in an attempt to conserve water. Above 15% soil moisture the plant was not affected, and below this threshold its g_s and A declined steadily as soil moisture was depleted. Smaller stomatal apertures reduced its ability to uptake CO_2, which is evident in the declining A. Smaller stomatal apertures do not, however, explain the declines observed in I_e. Past research has shown that mild drought stress has little effect on I_e, which was observed in the previous experiments (section 4.2.) as well (Pegoraro et al., 2004; Sharkey and Loreto, 1993; Guenther et al., 1999). Thus, the observed decline in I_e was more likely due to the senescence as a result of the stresses placed on the seedling (Geron et al., 2000; Goldstein et al., 1998).

Figure 20. A *Q. alba* seedling before (A) and after (B) the drought + ozone experiment.

The amount of ozone taken up by the stomata was affected by the declining stomatal conductance. Figure 19 shows the decline in stomatal ozone uptake as a function of g_s; this relationship suggests the protective role drought may play in reducing damage incurred from ozone exposure (Panek and Goldstein, 2001; Panek, 2004). Drought encourages the plant to close its stomata, and this reduces the amount of ozone that enters the stomata, which could lead to a reduction in damage due to ozone. This relationship existed below a threshold of g_s, while above that threshold no effect on stomatal ozone uptake was noted. In this experiment, the threshold was at approximately 15 mmol m^{-2} s^{-1}. This effect can also be seen in the ozone deposition velocities shown in figure 18; the threshold was reached around days 8 – 9, after which deposition velocities declined steadily. A 'protective role' drought can play against ozone damage has been documented by Löw et al. (2006), however in their meta-analysis Wittig et al. (2009) found no definitive role of drought protecting against ozone damage. While a reduction in ozone entering the stomata was measured, the declines in the productivity, likely due to senescence, were large enough to overshadow any detectable 'protective role.'

4.4. *Quercus virginiana* ozone exposure

4.4.1. *Quercus virginiana* ozone exposure introduction

For this experiment, a Live oak (*Quercus virginiana*) seedling was exposed to a diurnal cycle of ozone, to determine its effects on physiology and the rate of stomatal uptake of ozone. This seedling had a one-sided leaf area of 0.0741 m^2. Prior to performing this experiment, this seedling had been treated with the same aphid mixture

as described in section 4.2.1. (*Q. alba* ozone exposure). This was done to protect the seedling from damage via aphids, but similar to the White Oak experiment, it had a significant effect on the ozone fluxes to this seedling. A detailed discussion of this coating and the effects it caused exists in section 4.2. (*Q. alba* ozone exposure). The seedling was inserted in the chamber and allowed to acclimatize for several weeks prior to performing this experiment. The seedling was subsequently exposed to two levels of ozone (60 and 100 ppb) during the day. Exposure periods were six and eight days for each of the above-mentioned concentrations respectively. At the onset of this experiment, the seedling was under mild water stress, it was then well watered and allowed to dry out over the second half of the experiment. This permitted the measurements of its physiology and ozone uptake at a wide range of g_s values. Ozone fluxes were partitioned into leaf surface and stomatal fluxes as described above (see Methods section 3.2.), as well as with a new method as described in the results section below. Soil moisture reached as high as 32% on day 5, and declined to below 20% before re-watering on day 13.

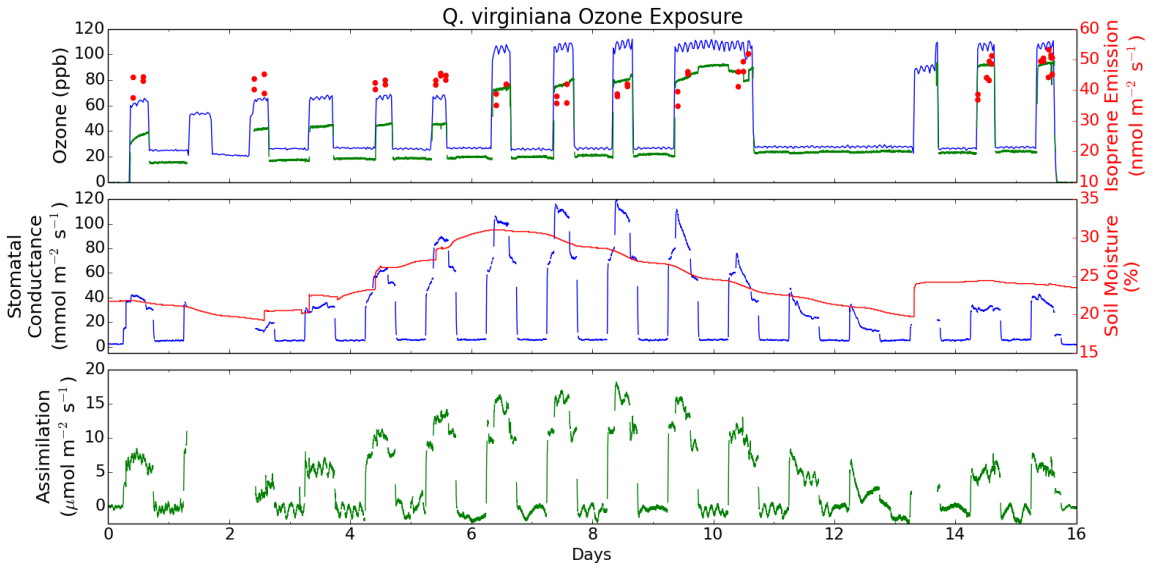

Figure 21. Timeline of ozone exposure experiment on *Q. virginiana*. Top panel shows incoming ozone (ppb) as a blue line, chamber ozone concentrations (ppb) as a green line, and isoprene emissions, I_e (nmol m^{-2} s^{-1}), as red dots. Middle panel shows stomatal conductance, g_s (mmol m^{-2} s^{-1}), as a blue line, and soil moisture (% by volume) as a red line. Bottom panel shows CO_2 assimilation, A (μmol m^{-2} s^{-1}), as a green line.

4.4.2. *Quercus virginiana* ozone exposure results

The wide range of g_s observed in this experiment as a result of manipulating the soil moisture had significant effects on A and stomatal ozone uptake during this experiment. Similar to the past drought experiments (see sections 4.1. and 4.3.), there was a strong correlation between A, gs, and soil moisture. g_s ranged from as low as 20 mmol m^{-2} s^{-1} at the beginning and end of the experiment (days 2 and 12, when it was water stressed), to as high as 110 mmol m^{-2} s^{-1} on day 8 ($p < 0.01$). A ranged from as low as 1.5 μmol m^{-2} s^{-1} on day 2 to as high as 18 μmol m^{-2} s^{-1} on day 8, and then declined to as low as 4 μmol m^{-2} s^{-1} on day 12. This represented an 81% change in g_s and a 91% change in A during this experiment ($p < 0.01$).

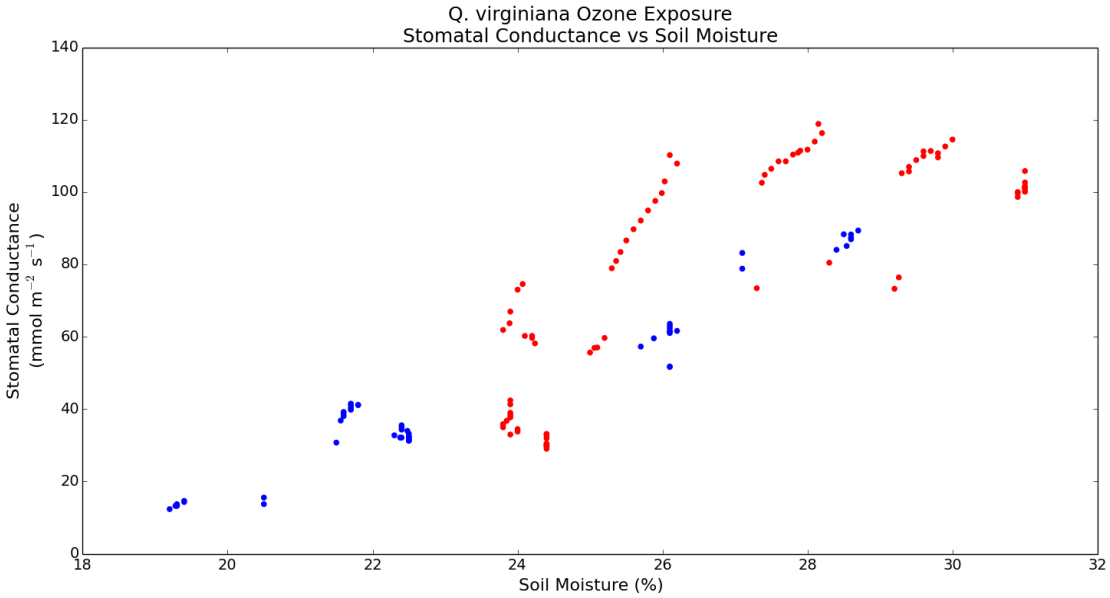

Figure 22. Relationship between stomatal conductance, g_s (mmol m^{-2} s^{-1}), and soil moisture (% by volume) for the *Q. virginiana* ozone experiment. Data represent daytime (11 am – 3 pm) 10-minute means for each half hour. Blue points represent data from the first half of the experiment (g_s rising with time and 60 ppb ozone). Red points represent data from the second half of the experiment (g_s declining with time and 100 ppb ozone).

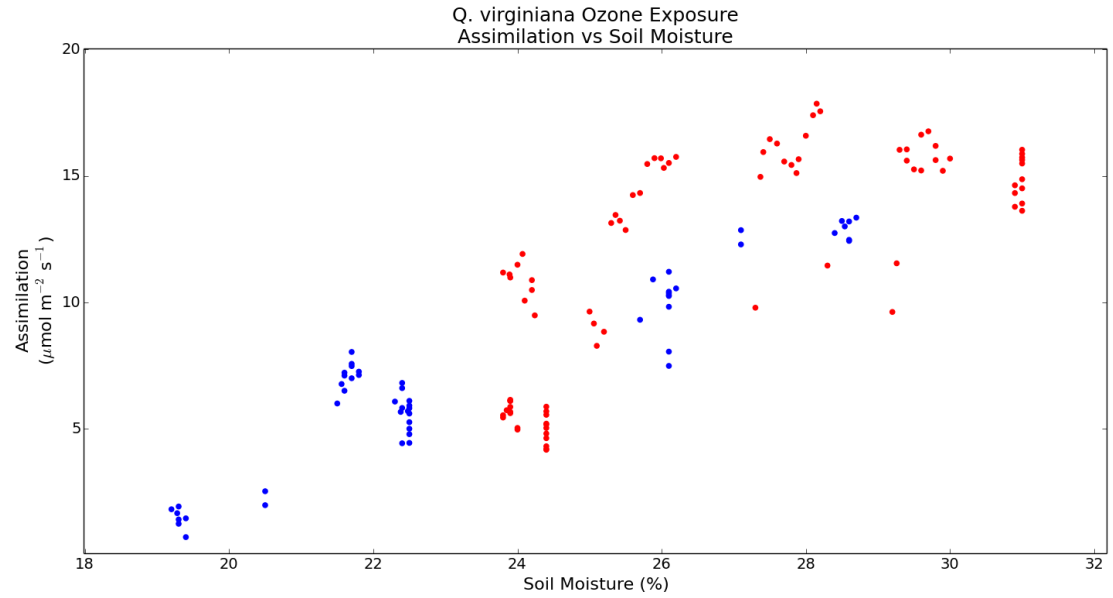

Figure 23. Relationship between CO_2 assimilation, A (µmol m^{-2} s^{-1}), and soil moisture (% by volume) for the *Q. virginiana* ozone experiment. Data represent daytime (11 am – 3 pm) 10-minute means for each half hour. Blue points represent data from the first half of the experiment (A rising with time and 60 ppb ozone). Red points represent data from the second half of the experiment (A declining with time and 100 ppb ozone).

No effects on I_e were detected during this experiment; I_e remained within its baseline range of variability of 35 – 55 nmol m^{-2} s^{-1} ($p > 0.05$). Additionally, no significant concentrations of MACR or MVK were detected, which would have resulted from gas phase reactions of ozone with isoprene.

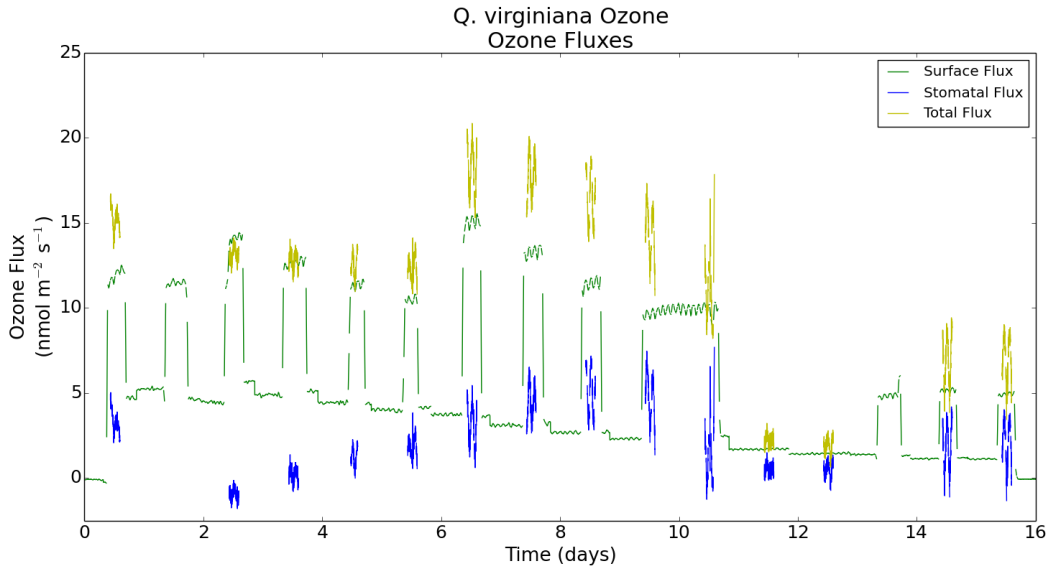

Figure 24. Plant ozone fluxes (nmol m^{-2} s^{-1}) during the *Q. virginiana* ozone experiment. Total plant fluxes are represented by a yellow line, plant surface fluxes are represented by a green line, and stomatal fluxes are represented by a blue line.

Because of the coating applied to the leaves, it was likely that the surface sink was larger than on an untreated specimen of this species. In this experiment, the surface sink appeared to change in the time frame of the experiment (note nighttime ozone differences between chamber and incoming ozone in figure 21). This occurred because the surface sink was being oxidized over time throughout the experiment. Further evidence of this exists in the experiment performed with a paper coated in the isoprenoid

mixture. The size of the sink on the paper diminished over time, likely similarly to the sink in this *Q. virginiana* experiment. As a result of this, the method used to estimate ozone fluxes used in previous experiments yielded negative (non-physical) stomatal ozone fluxes. The period designed to estimate leaf surface fluxes was halfway through this experiment (night 9-10), and as a result it underestimated the surface sink early in the experiment, and overestimated this sink later in the experiment.

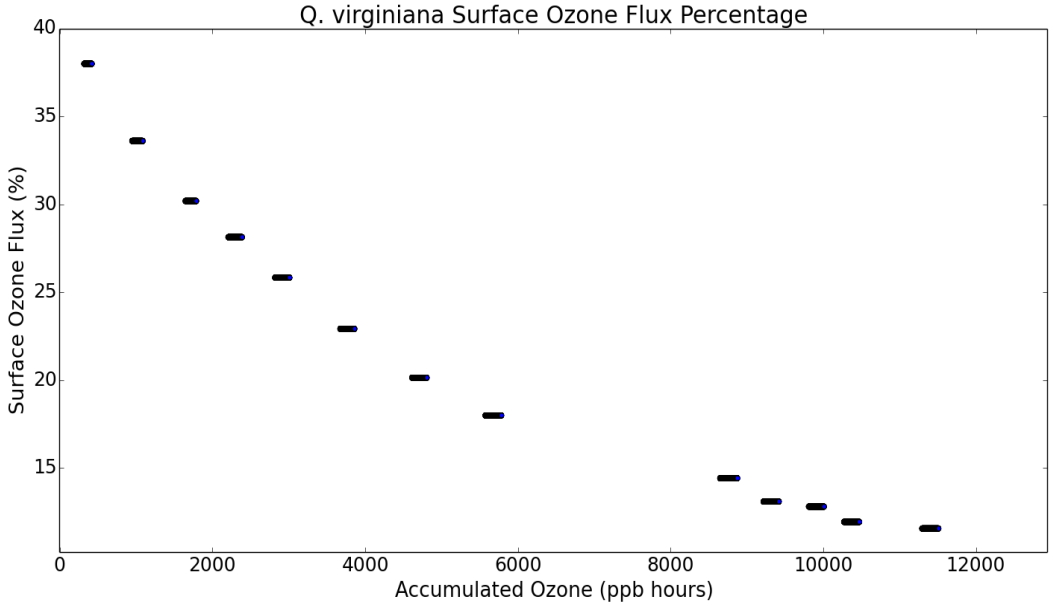

Figure 25. Relationship between accumulated ozone (ppb•hours) and fraction (%) of ozone fluxes going to plant surfaces during the *Q. virginiana* ozone experiment.

To remedy this, a new surface uptake was calculated each night during this experiment. This accounted for the highly transient nature of the surface ozone sink in this experiment. The rate recorded in the paper experiment (-1.614×10^{-3} % (ppb•hour)$^{-1}$) was used, however it was not large enough to eliminate the negative (non-physical) stomatal fluxes. It was found that surface fluxes rapidly decreased early in the experiment, at a

rate of -7×10^{-3} % $(ppb\bullet hour)^{-1}$ early in the experiment, and decreased to as little as -3.2×10^{-4} % $(ppb\bullet hour)^{-1}$ by the end of the experiment (figure 25). Results of this adjustment can be seen in figure 27, and after the adjustment, a clear relationship between g_s and stomatal ozone fluxes emerged.

Stomatal ozone fluxes ranged from near zero at the beginning and end of this experiment (when the seedling was water stressed) to as much as 18 nmol m^{-2} s^{-1} while it had wide open stomata at the midpoint of the experiment. Surface fluxes ranged from 5 to 15 nmol m^{-2} s^{-1}. Deposition velocities to surfaces were initially high, at 0.8 cm s^{-1} and declined to as low as 0.1 cm s^{-1} by the end of the trial (figure 26). This was due to the rate at which the coating was oxidized, and the resulting change in surface fluxes calculated each night. Stomatal deposition velocities followed a similar pattern as g_s during this trial; they were low at the beginning and end of the experiment, and peaked near the midpoint when g_s was highest. Stomatal deposition velocities ranged from near zero early in the experiment to a maximum of 0.15 cm s^{-1} on day 8 (figure 26).

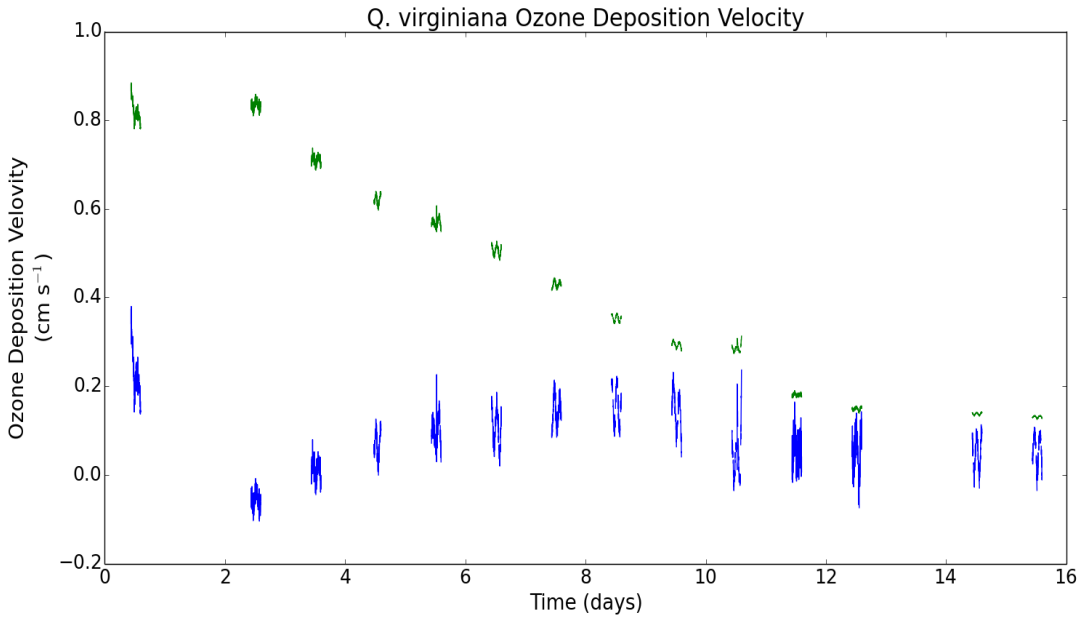

Figure 26 Ozone deposition velocities (cm s^{-1}) for the *Q. virginiana* ozone experiment. Stomatal deposition velocities are represented by a blue line, and surface deposition velocities are represented by a green line. Data represent daytime (11 am – 3 pm) values only.

4.4.3. *Quercus virginiana* ozone exposure discussion

Because of the large deviations in productivity during this experiment due to the manipulation of soil moisture, no definitive conclusions about ozone affecting the seedling's productivity could be drawn. The effects of water stress and oversaturation outweighed any ozone-caused impacts on the plant's physiology. When the seedling's mineral soil became oversaturated during the first half of the experiment, it responded by opening its stomata widely, maximizing transpiration. These large stomatal apertures resulted in elevated A, and likely overshadowed any measurable effects on productivity due to ozone. Similarly, as the specimen became increasingly water stressed during the second half of the experiment, it displayed significant reductions in its productivity due to reduced stomatal apertures. This experiment resulted in much larger changes in g_s

due to changing soil moisture compared to the *Q. alba* experiments. The response in this case was ten times the magnitude of the *Q. alba* experiments (9.0 mmol m^{-2} s^{-1} (% Soil moisture)$^{-1}$ compared to 0.86 mmol m^{-2} s^{-1} (% Soil moisture)$^{-1}$ for *Q. alba*), which represented a significantly higher degree of stomatal control for this species.

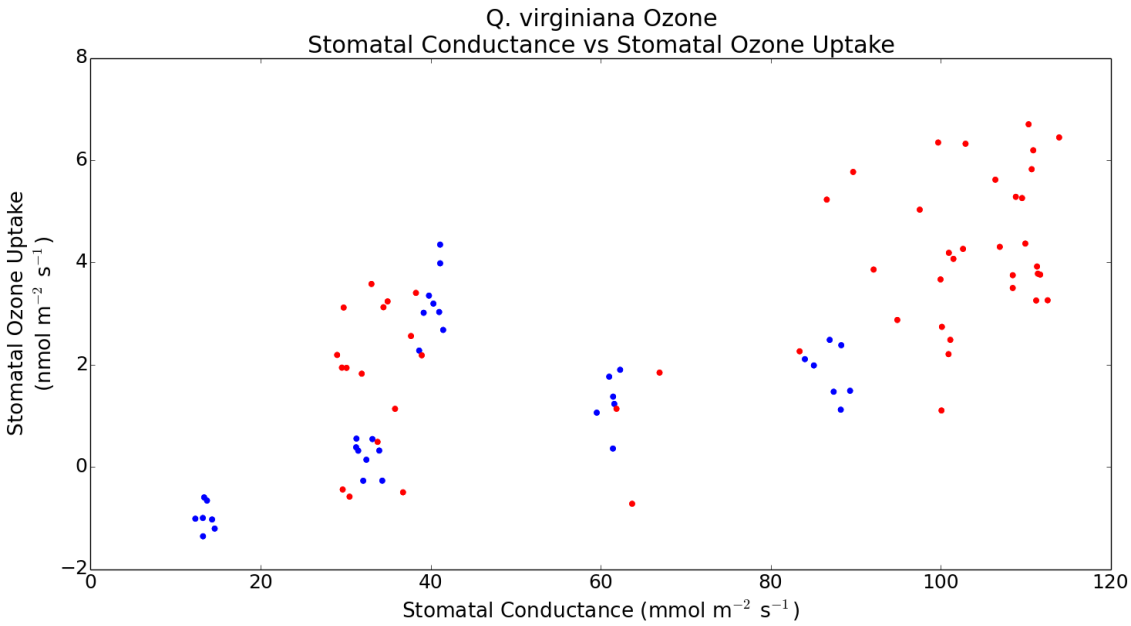

Figure 27. Relationship between stomatal conductance, g_s (mmol m^{-2} s^{-1}), and stomatal uptake of ozone (nmol m^{-2} s^{-1}) for the *Q. virginiana* ozone exposure experiment. Data represent daytime (11 am – 3 pm) 10-minute means for each half hour during ozone exposure. Blue dots represent data from the first half of the experiment (g_s rising over time and 60 ppb ozone). Red dots represent data from the second half of the experiment (g_s declining over time and 100 ppb ozone).

This specimen experienced a wide range of fluxes of ozone via the stomata due to the changing g_s. Unlike the *Q. alba* I ozone experiment with coated leaves, this specimen had significant stomatal ozone uptake despite the coating applied to the leaves. Measurements in the *Q. alba* experiment indicated that this coating removed ozone at the leaf boundary layer, and as a result reduced the magnitude of the ozone gradient across the stomata. This effect did not dominate stomatal fluxes in this experiment

however. Because some stomatal fluxes of ozone were detected, and no MACR or MVK, I conclude that the majority of this flux was going to surfaces within the leaf and not to gas phase reactions with isoprene. If it were reacting with isoprene in the intercellular spaces in significant amounts, it would likely have been possible able to detect reaction products.

Unlike the *Q. alba* drought + ozone experiment, stomatal ozone fluxes responded to changes in g_s throughout the entire range of measured g_s. As the stomata opened during the experiment, significant fluxes of ozone occurred to the stomata, and as the stomata closed the stomatal flux of ozone reduced significantly ($p < 0.01$). This relationship suggests the protective role drought may play in reducing damage incurred from ozone exposure (Panek and Goldstein, 2001; Panek, 2004). In the *Q. alba* experiment, a threshold was identified of approximately 15 mmol m^{-2} s^{-1}, above which changing g_s did not affect stomatal ozone uptake. There are several possible explanations for this. It is possible that this threshold does not apply to all species; either *Q. virginiana* has a threshold above the measured g_s in this experiment, or this species does not have such a threshold at all. A more likely explanation is that the single *Q. alba* experiment misidentified a threshold where there should not be one, or that further experiments with *Q. virginiana* would reveal a threshold. Further study will be needed to confirm the presence of this threshold to a significant confidence level.

4.5. *Quercus muehlenbergii* ozone exposure

4.5.1. *Quercus muehlenbergii* ozone exposure introduction

For this experiment, a Chinkapin oak (*Quercus muehlenbergii*) seedling was exposed to a diurnal cycle of ozone, as described above (section 4.2.), to determine its effects on plant physiology and the rate of stomatal uptake of ozone. This seedling had a one-sided leaf area of 0.280 m^2 at the onset of the experiment, and at the end had a leaf area of 0.231 m^2 due to both growth and the removal of selected leaves. The seedling was placed in the chamber and allowed to acclimatize for several weeks prior to performing this experiment. The seedling was exposed to three levels (40, 60, 90 ppb) of incoming ozone during the day. Exposure periods were 7, 9, and 5 days for each of the above-mentioned concentrations respectively. Figure 28 shows the timeline of this experiment, with days 1-7 at 40 ppb daytime ozone, days 8-16 at 60 ppb, and days 17-21 at 90 ppb. For three nights (nights 3, 10, 19), one for each daytime concentration, the ozone was left elevated overnight to better estimate the rate of leaf surface ozone removal within the chamber. In addition to monitoring ozone fluxes within the chamber, for this experiment several leaves were removed to assess their reactive oxygen species (ROS) content (not shown). Removed leaves' areas were measured using the technique described in the methods section above (section 3.1.), and were added to the final leaf area measurements for data prior to the time of removal.

The seedling was monitored for effects on its physiology by measuring rates of A and g_s, as well as measuring its emissions of isoprene. Levels of MACR and MVK were monitored within the chamber, as they are products of the reaction of isoprene with

ozone. An upper estimate of 0.25 ppb MACR was made based on the maximum observed ambient concentrations of 61 ppb ozone and 55 ppb isoprene. This estimate was compared to the measured concentrations to determine whether ozone entering the stomata led to significant amounts of MACR and MVK formation from reactions with isoprene in the stomatal cavities of the leaves.

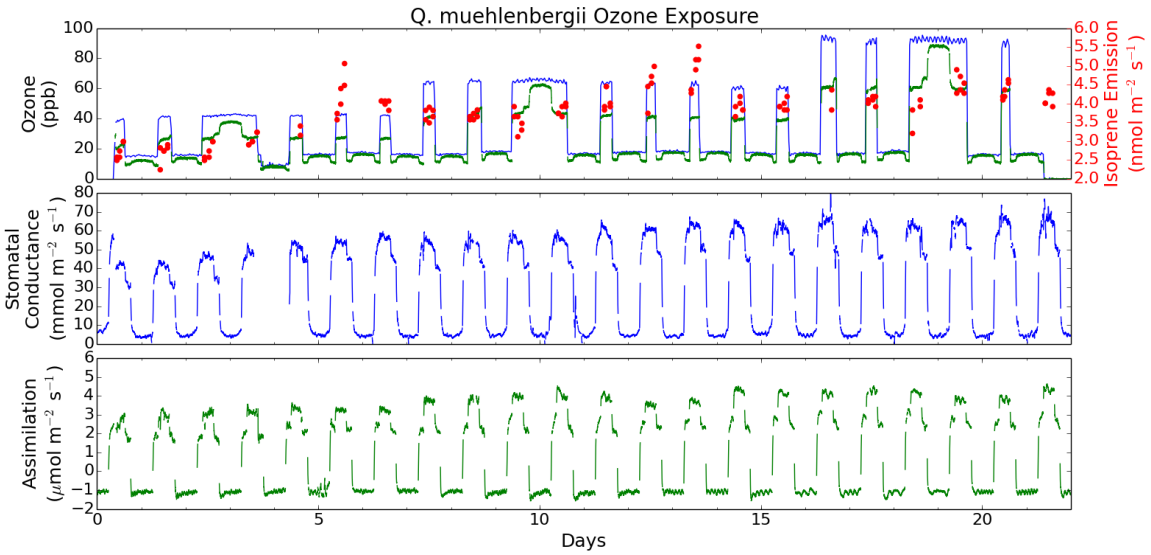

Figure 28. Timeline of ozone exposure experiment on *Q. muehlenbergii*. Top panel shows incoming ozone (ppb) as a blue line, chamber ozone concentrations (ppb) as a green line, and isoprene emissions, I_e (nmol m^{-2} s^{-1}), as red dots. Middle panel shows stomatal conductance, g_s (mmol m^{-2} s^{-1}), as a blue line. Bottom panel shows CO_2 assimilation, A (μmol m^{-2} s^{-1}), as a green line.

4.5.2. *Quercus muehlenbergii* ozone exposure results

No detrimental effects on the *Q. muehlenbergii* seedling's productivity was detected as a result of ozone exposure. This particular experiment was performed in spring, so the seedling was actively growing at the time (through both leaf and stem expansion), thereby increasing its transpiration and assimilation rates over time. This increasing trend can be seen in Figure 28, represented by day to day increases in g_s and

overall increases in A. g_s increased from 40 mmol m^{-2} s^{-1}, to as high as 70 nmol m^{-2} s^{-1} (75% increase; $p < 0.01$), and A increased from 2.7 µmol m^{-2} s^{-1}, to as high as 4.9 µmol m^{-2} s^{-1} (44% increase; $p < 0.01$). I_e also increased during this period, from an initial 2.5 nmol m^{-2} s^{-1}, to as high as 5 nmol m^{-2} s^{-1} at the end of the experiment (100% increase; $p < 0.01$). In addition to the overall increasing trend in I_e during this experiment, there was a periodic cycle of I_e, with peaks occurring on days 5, 13, and 19. Possible explanations for this periodicity are discussed below.

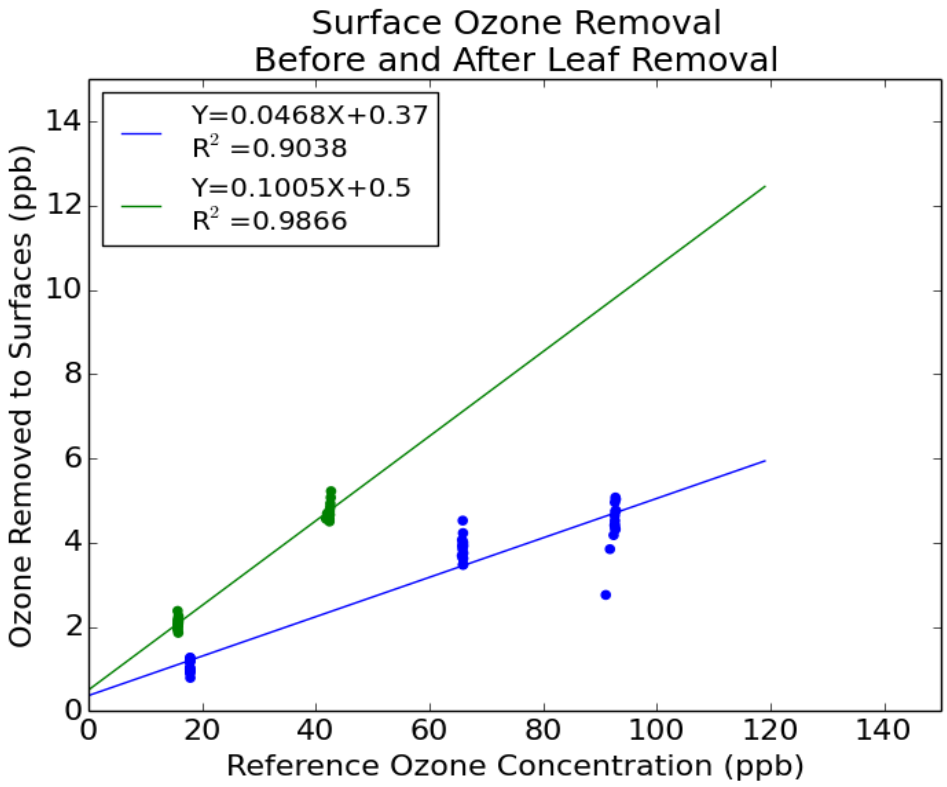

Figure 29. Relationship between incoming ozone reference (ppb), and amount of ozone removed to surfaces (Δ ppb) for the five nights at varying concentrations. Data represent nighttime (10 pm – 4 am) 10-minute means for each half hour. Green and blue points represent data recorded before and after removing leaves for ROS analysis, respectively.

Ozone fluxes in the chamber were partitioned into stomatal and surface fluxes. Gas phase fluxes of ozone, via reactions with isoprene and assessed by measuring concentrations of MACR and MVK formation within the chamber, were not detected. Concentrations of MACR and MVK within the chamber did not vary significantly compared to samples taken of incoming air (not shown).

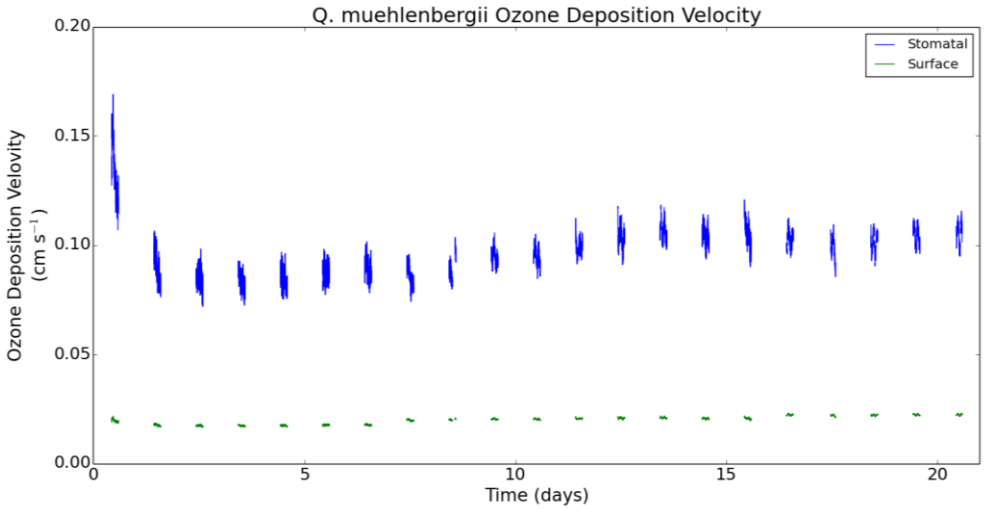

Figure 30. Ozone deposition velocities (cm s^{-1}) for the *Q. muehlenbergii* ozone experiment. Stomatal deposition velocities are represented by a blue line, and surface deposition velocities are represented by a green line. Data represent daytime (11 am – 3 pm) values only.

Estimates of surface ozone fluxes within the chamber were made based on nighttime ozone fluxes at several incoming concentrations. Figure 29 shows the fraction of ozone removed to surfaces during this experiment; before removal of leaves for ROS analysis approximately 10% of incoming ozone was removed to surfaces, while after the temporary opening of the chamber to remove leaves a lower amount of approximately 5% of incoming ozone was removed to surfaces. Because of complications with the chamber during this experiment, the data in Figures 29-32 represent the total surface flux

(chamber and plant surfaces). Stomatal fluxes were estimated by assuming that the only other sink for ozone in the chamber, aside from the above mentioned total surface fluxes, would be via the plant's stomata. The stomatal flux was between 1.1 and 3.3 nmol m^{-2} s^{-1}, which represented between 80 to 85% of the total flux. Surface fluxes for this experiment were between 0.2 and 0.5 nmol m^{-2} s^{-1}, which represented between 15 to 20% of the total flux (figure 32). The stomatal fraction remained consistent throughout the experiment, despite changing incoming concentrations (figure 31). As can be seen in figure 28, there was almost no difference between incoming and chamber ozone at night when the stomata were closed, indicating negligible stomata ozone fluxes.

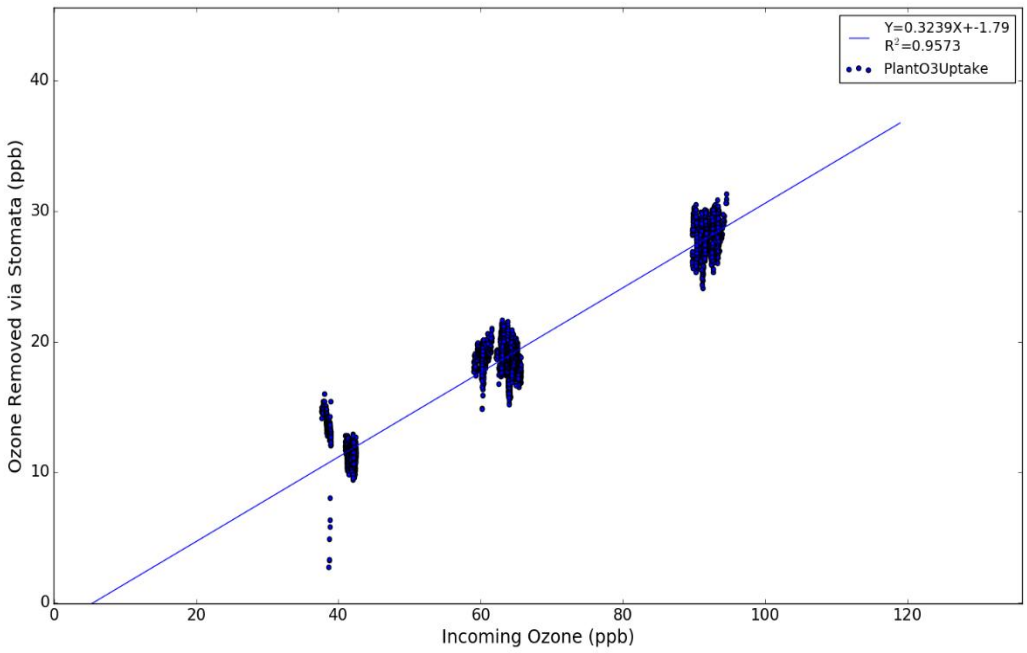

Figure 31. Relationship between incoming ozone reference (ppb), and amount of ozone removed via stomata (Δ ppb) throughout the *Q. muehlenbergii* ozone experiment. Data represent daytime (11am – 3 pm) 10-minute means for each half hour.

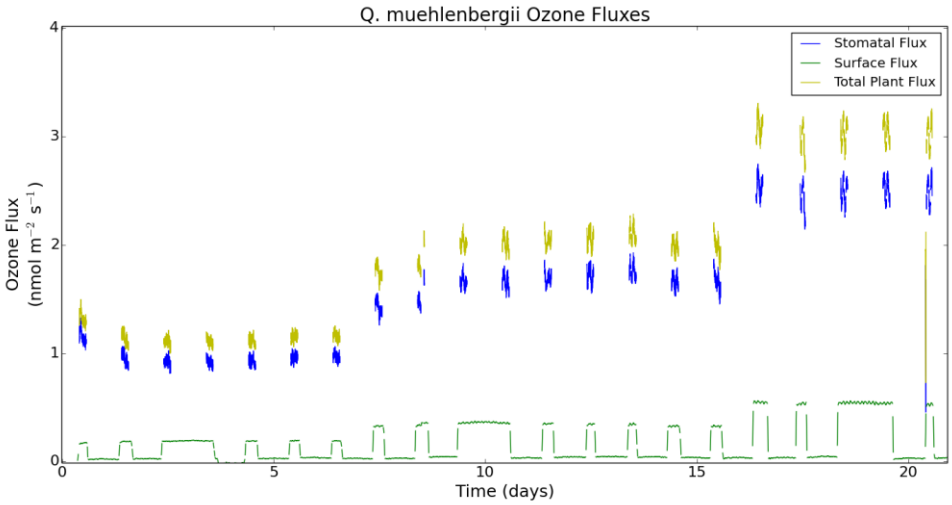

Figure 32. Plant ozone fluxes (nmol m^{-2} s^{-1}) during the *Q. muehlenbergii* ozone experiment. Total plant fluxes are represented by a yellow line, plant surface fluxes are represented by a green line, and stomatal fluxes are represented by a blue line.

4.5.3. *Quercus muehlenbergii* ozone exposure discussion

Throughout this experiment, there was no evidence of detrimental effects on the plant's physiology due to ozone exposure. This was likely due to the growth of the seedling at the time of the experiment. This growth had positive effects on g_s and A, which likely overshadowed any negative effects due to ozone exposure. No negative effect on I_e was noted, and similar to g_s and A, it displayed an overall increase, likely in large part due to the growth of the tree at its top (increasing leaf area exposed to high light levels). The periodic pattern of I_e seen in figures 28 and 33 with a period of 7-10 days could have several explanations. One possible explanation was due to the removal of leaves for ROS analysis. This removal of leaves resulted in lower-canopy leaves becoming exposed to higher light levels. Over the next few days, these newly exposed

leaves responded by increasing their I_e. This could explain the pattern, as leaves were removed on day 0 and day 8, which could result in the noted 7-10 period of I_e oscillations. Another explanation is based on the leaf temperatures within the chamber. Temperature was not directly controlled in the chamber, but remained relatively stable because the chamber resides in a climate controlled laboratory. Changes in daytime maximum temperature within the chamber of around 1-2 °C were observed. I_e responds strongly to temperature, and as can be seen in figure 33, isoprene emission was well correlated with the mean leaf temperatures during this time. In future experiments, it may be beneficial to explicitly control the temperature in the chamber. This would remove this variable and allow the isoprene measurements to be better comparable to other studies.

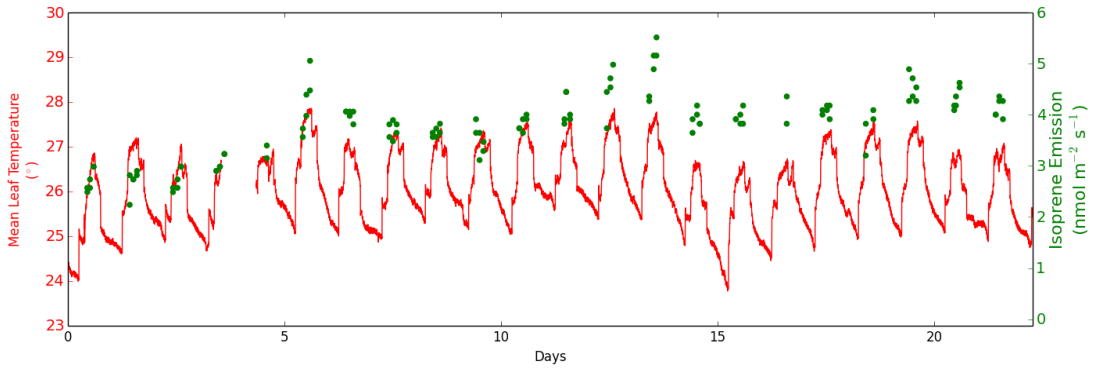

Figure 33. Timeline of mean leaf temperature (°C) and isoprene emission, I_e (nmol m^{-2} s^{-1}), during the *Q. muehlenbergii* ozone exposure experiment. Leaf temperatures represent an average of three leaf temperature sensors placed on three leaves at the top, middle and bottom of the seedling.

The fact that the fraction of incoming ozone removed via stomata (figures 31 and 32) was relatively constant, despite the removal of several leaves mid experiment, has several implications: the leaves responsible for the stomatal fraction of ozone flux are

not equally distributed across the plant; the removed leaves were taken from within the canopy, i.e. not sun leaves, and this was done in an attempt to preserve the productivity of the plant while assessing ROS during the ozone exposure. However, these leaves were seemingly acting as significant source of surface reactions of ozone, as evident in the change in surface removal depicted in figure 29. The removed leaves were of low activity with respect to g_s, A, or I_e as is evident in the small change in these parameters in figure 28 on day 8 when the leaves were removed. This indicated that the removed leaves likely had small stomatal conductance to CO_2, H_2O, and ozone, and low isoprene emission capacity, as compared to the bulk of the leaves. This can be explained by the fact that the leaves removed from lower on the stem were "old" leaves from the prior growth season, which are less photosynthetically active; in addition, they had been treated with the aphid mixture, which can in part explain the change in surface fluxes. Furthermore, the low conductance finding agrees with findings in the *Q. alba* drought + ozone experiment: leaves below a threshold of g_s are less efficient at removing ozone. It is likely that the leaves removed were below the threshold for this species. This gives rise to the hypothesis that in nature, there are only a portion of leaves strongly affected by ozone exposure in the form of stomatal uptake of ozone, namely the leaves with high stomatal conductance which are effectively 'pumping' ozone through their stomata (see also dominant discoloration of light-exposed leaves in Figure 20 from section 4.3.). This in turn supports the hypothesis that isoprene emission evolved as protection against oxidants, as its emission is collocated in the canopy with leaves which have elevated ozone uptake via stomata.

4.6. *Quercus muehlenbergii* circadian control

4.6.1. *Quercus muehlenbergii* circadian control introduction

The level of circadian control on physiology and I_e was assessed for the same *Q. muehlenbergii* seedling mentioned above. This seedling had a one-sided leaf area of 0.280 m^2. Prior to these experiments, the seedling was installed in the chamber and allowed several weeks to acclimatize to the conditions within. The standard lighting conditions during this time were 12 hours of light and 12 hours of darkness. Half the lights turned on at 7 am, then all lights turn on from 11 am to 3 pm, then half lights are on until 7 pm. After this period, baseline measurements were taken, including a period of 48 hours when around the clock VOC samples were taken (figure 34, days 1-3). This was done to establish a typical diurnal cycle for the seedling's I_e. To determine the level of circadian control, the lights were left on for several days continuously. This was repeated twice, once for two nights, and then again for four nights (figure 34 days 7-9 and 20-24). During these intense observation periods (IOP) isoprene measurements were taken approximately every four hours, as opposed to the typical three times a day (daytime only) regime. In between the IOPs, the seedling was allowed to recover for 10 days to allow g_s, A, and I_e returned to their baseline values.

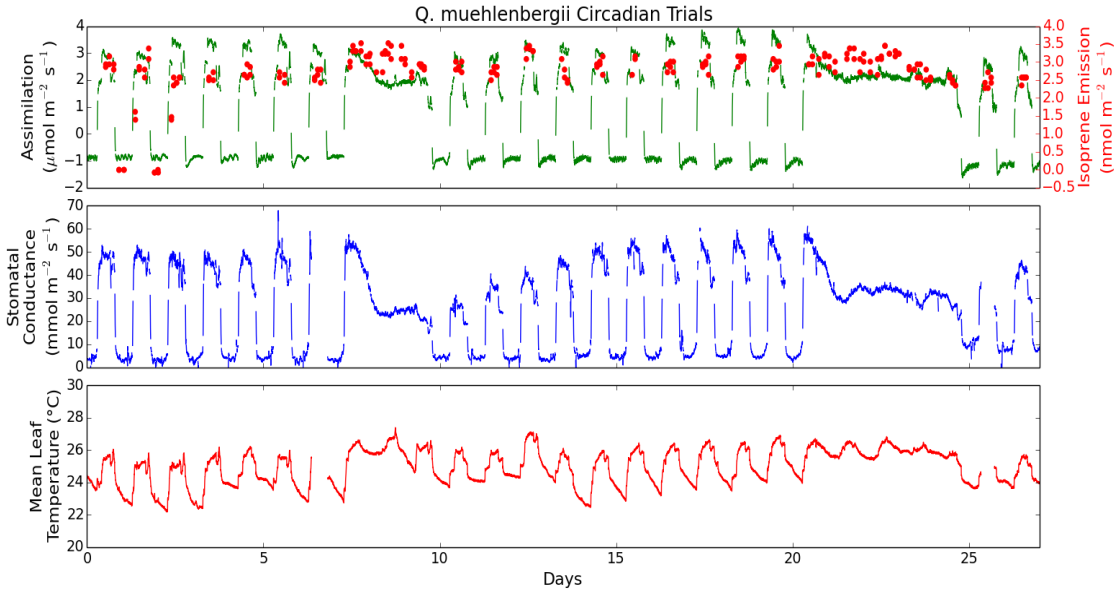

Figure 34. Timeline of circadian control experiment on *Q. muehlenbergii*. Top panel shows CO_2 assimilation, A (μmol m^{-2} s^{-1}), as a green line, and isoprene emissions, I_e (nmol m^{-2} s^{-1}), as red dots. Middle panel shows stomatal conductance, g_s (mmol m^{-2} s^{-1}), as a blue line. Bottom panel shows mean leaf temperature (°C) as a red line.

4.6.2. *Quercus muehlenbergii* circadian control results

During the baseline measurements, daytime maximum values of 52 mmol m^{-2} s^{-1}, 3.5 μmol m^{-2} s^{-1}, and 3.5 nmol m^{-2} s^{-1} were recorded for g_s, A, and I_e respectively. Morning samples of isoprene, at times when half the lights were on, yielded reduced emissions of isoprene; values of 1.6 nmol m^{-2} s^{-1} were measured for I_e at this time. As expected, during lights-off conditions, no isoprene emissions were recorded from the seedling. Values of zero for g_s and approximately -1.0 μmol m^{-2} s^{-1} for A were recorded due to leaf respiration. This indicated a strong light dependence for all these variables, as expected, and can be seen in the timeline of the baseline measurements on days 0-3 (Figure 34).

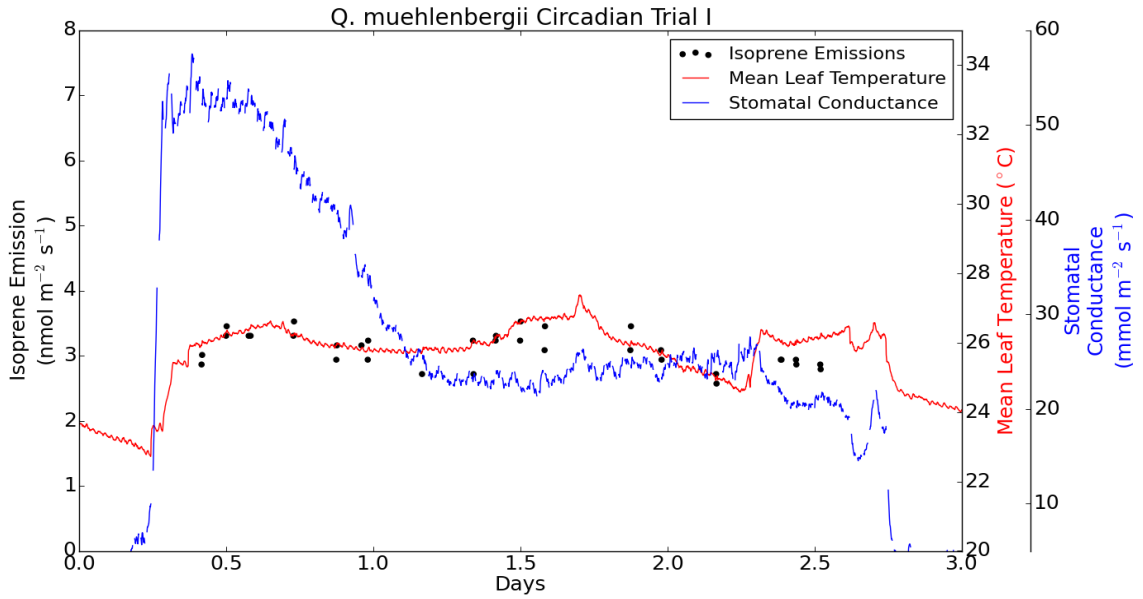

Figure 35. Timeline of the first circadian control experiment on *Q. muehlenbergii*. The left axis has isoprene emissions, I_e (nmol m^{-2} s^{-1}), as black points. The near right axis has mean leaf temperatures (°C) as a red line, and the far right axis has stomatal conductance, g_s (nmol m^{-2} s^{-1}), as a blue line.

During the first experiment, both A and g_s gained their typical daytime maximum on the first day, however they declined steadily as the experiment continued into the first night (Figure 35). By the end of the lights-on period, A had declined to as low as 2.5 µmol m^{-2} s^{-1}, down from a maximum of 3.1 µmol m^{-2} s^{-1} on the first day. g_s displayed a stronger decline as the experiment progressed; it declined to as low as 20 mmol m^{-2} s^{-1} after reaching a peak of 56 mmol m^{-2} s^{-1} on the first day. These represented declines of 63% for g_s and 20% for A compared to their peaks on day one of this IOP ($p < 0.01$). A weak periodic cycle of I_e was recorded, with a period of approximately 24 hours, as can be seen in figure 35, denoted with peaks near 0.6 and 1.6 days into the experiment. These oscillations were only significant to a level of $p < 0.1$; the small deviations

responsible for this pattern were likely due to temperature fluctuations within the chamber. There was a regular 24-hour temperature pattern in the chamber, and while this was reduced during the continuous lights on IOP's, it was not removed entirely. There was a significant ($p < 0.01$) periodicity to g_s during this experiment, however the second 'peak' did not occur until day 2 of the experiment (figure 35). The pattern of g_s did not display a 24-hour period (i.e. not in phase with temperature fluctuations), which indicates that it is more likely to be caused by the plant's own circadian control rather than the temperature fluctuations in the chamber. A further discussion of these patterns is made in the following section. During the second experiment, where the IOP was extended to four nights, the periodic cycles overall were more pronounced.

During the second lights-on period, depicted in Figure 36, the seedling again displayed typical daytime maximum values for I_e, A, and g_s on the first day, and then declined steadily as the experiment continued. By the end of the experiment, levels of g_s, A, and I_e reached as low as 27 mmol m^{-2} s^{-1}, 2.0 μmol m^{-2} s^{-1}, and 2.2 nmol m^{-2} s^{-1} respectively. These represented declines of 50%, 42%, and 26% for g_s, A and I_e respectively ($p < 0.01$). Along with the steady decline of these parameters, a periodic cycle in g_s and I_e was noted as well. Figure 36 shows this cycle, with peaks in I_e every 24 hours, however this pattern was only significant during the second two oscillations (figure 36: days 1.5 – 3.5) to the level of $p < 0.05$. I_e was well correlated with the mean leaf temperature during these experiments, which likely explains the reason for its diurnal pattern.

A circadian control over g_s was detected during the second experiment as well. The significant ($p < 0.01$) diurnal pattern displayed by the g_s was not well correlated with the mean leaf temperature as seen with I_e. There is most likely a circadian control being expressed by the plant to cause this pattern of stomatal opening and closing. The period of these oscillations did not appear to be constant, as times between peaks in g_s were 37, 18, and 32 hours apart during the second experiment. There was not an evident circadian cycle of A, either due to the 24-hour temperature fluctuations, or due to any circadian control expressed by the plant in either experiment (not shown; $p > 0.05$).

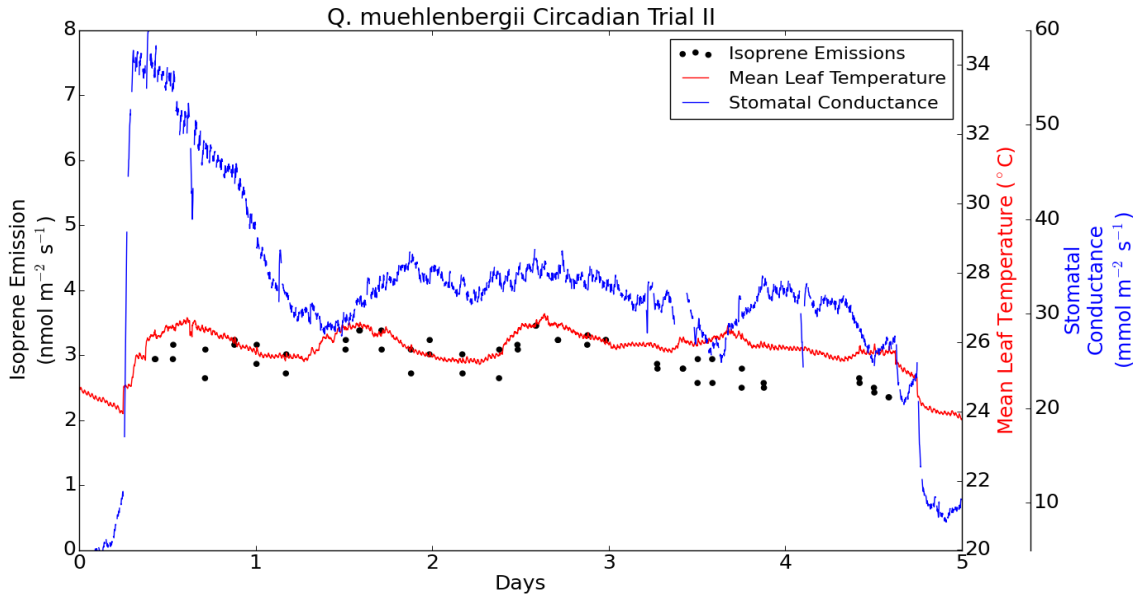

Figure 36. Timeline of the second circadian control experiment on *Q. muehlenbergii*. The left axis has isoprene emissions, I_e (nmol m^{-2} s^{-1}), as black points. The near right axis has mean leaf temperatures (°C) as a red line, and the far-right axis has stomatal conductance, g_s (nmol m^{-2} s^{-1}), as a blue line.

4.6.3. *Quercus muehlenbergii* circadian control discussion

While I_e did display a diurnal cycle, it was likely due to temperature fluctuations, since it was well correlated with the mean leaf temperature and isoprene emissions are strongly temperature dependent. For this reason, I think it is likely that *Q. muehlenbergii* does not have circadian control over isoprene emissions. Similar experiments into circadian control of isoprene emission of oil palm (Wilkinson et al., 2006) and grey poplar (Loivamaki et al., 2007) has shown fluctuations of I_e up to 90%. This was not the case with the *Q. muehlenbergii* seedling in this work. Further investigation into the circadian control of I_e for this species would be needed to better understand this process. Because significant diurnal mean leaf temperature fluctuations were present, it would be beneficial to directly control the temperature in the chamber. This would remove that variable as a possible stimulus for the observed diurnal cycles. It would also be beneficial to perform similar experiments on other *Quercus* species, as well as some mature *Quercus* specimens.

A diurnal cycle was observed in g_s for these experiments, and because it was not in phase with the leaf temperature fluctuations, it is likely that this cycle was due to circadian control by the plant. In addition to a periodic cycle of g_s, it declined steadily as the experiments continued. This was observed in past constant-light experiments as well (Wilkinson et al., 2006; Loivamaki et al., 2007). No measurable fluctuations in A were observed, despite minor temperature-induced fluctuations in I_e; this indicated a decoupling of these two metabolisms. This decoupling was noted in past circadian control experiments as well, however it was not as significant because the I_e fluctuations

recorded here were not as pronounced as those noted by Wilkinson et al. (2006) and Loivamaki et al. (2007).

5. SUMMARY

For this work, several species of oak seedlings were tested in a laboratory chamber to assess their vulnerability to drought and high external ozone concentrations. The oaks used (*Quercus alba, Quercus muehlenbergii* and *Quercus virginiana*) were all emitters of the volatile organic compound isoprene. Isoprene (C_5H_8) represents the largest individual emission (5×10^{14} g yr^{-1}) among biogenic terpene emissions, however the reasons for plants to produce isoprene is not fully understood (Guenther et al., 2006). Studies have shown that isoprene can provide enhanced thermotolerance (Sharkey and Yeh., 2001; Velikova and Loreto, 2005) and protection from ROS damage (Sharkey 2005; Jardine et al., 2012; Loreto et al. 2001). Isoprene emissions, along with several physiological parameters (stomatal conductance, transpiration, assimilation) were monitored in a controlled chamber setting during drought simulations and high external ozone.

The motivation for this work was to better elucidate the response of isoprene emissions and physiological responses to stressful climactic events. Climate models project increased severity of drought over the next century, which will have profound effects on plants and crop yields (IPCC 2013 report). Because isoprene is a large contributor to atmospheric chemistry on a global scale, it is important to understand how drought and climate change will affect these emissions (Folberth et al., 2006; Dreyfus et al., 2002; Sharkey and Yeh, 2001). In addition to drought, the impact of ozone on plants' productivity and isoprene emissions was examined. Projections of ozone concentrations are somewhat uncertain. Depending on anthropogenic emissions of

ozone precursors, the atmospheric load of ozone could increase in the coming century (IPCC 2013 report). Understanding ozone's effect on plant productivity and its interaction with isoprene are important because ozone has significant negative impacts on plant productivity and crop yields (Wittig et al., 2007). The interaction between surface and stomatal ozone uptake was examined in this work as well. Studies have shown that while the majority of ozone fluxes occur via stomatal uptake (Uddling et al., 2010; Fares et al., 2008), there are studies that have examined surface fluxes of ozone and have shown that these fluxes are significant (Jud et al., 2016; Laisk et al., 1989; Cape et al., 2009; Fares et al., 2010).

In this work, drought experiments, ozone experiments, and drought + ozone experiments were performed. In the drought experiments, it was noted that isoprene emissions were not affected despite significant reductions in stomatal conductance and assimilation. Significant reductions in assimilation in addition to near constant isoprene emissions led to changes in the percentage of assimilated carbon emitted as isoprene. Past research has shown that under normal conditions isoprene represents approximately 2% of assimilated carbon, and that under times of water stress this percentage can rise as high as 50% (Pegoraro et al., 2004; Sharkey and Loreto, 1993; Guenther et al., 1999). In this work a maximum of 4.4% of assimilated carbon was emitted as isoprene, up from 2.4% under non-stressed conditions. These results support the theory that while the majority of carbon used in isoprene synthesis comes from recently assimilated carbon, there appears to be an alternate pool of carbon for plants to use (Affek and Yakir, 2003; Karl et al., 2002).

In the drought + ozone experiments, a significant reduction in plant productivity was recorded. The *Quercus alba* specimen has significant reductions of stomatal conductance, assimilation, and isoprene emissions. These reductions represented an induced senescence caused by the combination of drought and ozone exposure.

Due to an outbreak of aphids in the lab, a treatment of olive oil, lavender oil, soap and water was applied to the leaves of the plants. This acted to control the aphid infestation, but it had significant effects on ozone uptake for some of the ozone exposure experiments. The coating contained isoprenoids from the lavender oil, which react readily with ozone (Munoz-Bermomeu et al. 2007). As a result, during some of the ozone exposure experiments, abnormally high ozone fluxes were recorded to the leaf surfaces that were treated with this coating. Due to the large removal of ozone at the surface of the leaves, ozone concentrations in the leaf boundary layer were reduced, which led to minimal ozone uptake into the stomata. Although it was not detected, it is likely that this reduction in stomatal ozone uptake reduced oxidative damage to the intercellular structures, and therefore mitigated ozone-induced reductions in productivity. For plants not treated with this mixture, stomatal ozone uptake was significantly higher. The *Quercus muehlenbergii* experiment (without the coating), stomatal uptake was as high as 30% of incoming ozone, while in a *Quercus alba* experiment with the 'protective' coating, stomatal uptake was undetectable. Throughout all ozone experiments, reaction products of ozone and isoprene were not detected. If ozone had entered the stomata in significant quantities and reacted with intercellular isoprene, it would have been possible to detect significant concentrations of

methacrolein. Because no methacrolein was detected, it is likely that even when significant stomatal ozone uptake was occurring, it was reacting with intercellular structures and not gaseous isoprene in the stomatal cavity.

Future work should be done to better understand some of the findings presented in this work. It would be beneficial to develop a method of maintaining a set temperature within the chamber. This would allow for temperature, which has a strong effect on isoprene emissions, to be explicitly controlled. A temperature controlled environment would allow the measurements taken in the chamber to be more directly comparable to other researchers' work. The scientific community generally attempts to measure these variables (isoprene emissions, photosynthesis, stomatal conductance etc.) at standard conditions. These standard conditions are at a set temperature, CO_2 concentration, and light level. If the chamber could be fine-tuned to be able to take standard measurements, this work would be more easily comparable to past research, and would therefore provide more utility to the scientific community.

This research was not able to measure a significant degree of circadian control over I_e for the *Q. muehlenbergii* seedling tested. There was a distinct correlation between temperature and isoprene emissions in the circadian control experiment, which could have overshadowed any circadian control on isoprene emissions expressed by the plant. If the chamber had a regulated temperature, this variable could be removed from this type of experiment, possibly allowing for a detectable signal of circadian control to be measured. It is possible that no clear circadian control over isoprene emissions was measured because an immature specimen was used, and circadian control is only

expressed by mature specimens of this species. To test this hypothesis, it would be necessary to perform experiments on large, mature plants, clones taken from mature trees, or even field-grown trees. If no circadian control were found, it would be useful to test other species in the *Quercus* genus to determine if this trait is found among all members.

Further work is also needed to assess the result of applying an isoprenoid coating to leaves during ozone exposure. I hypothesize that the coating provides some level of protection from ozone damage to the plant, and will therefore reduce ozone-caused reductions in productivity. To test this hypothesis, it would be necessary to perform replicates of this type of experiment to determine if the coating provided a significant level of protection. To achieve this, it would be useful to expose specimens to higher concentrations of ozone in the chamber, or use species more susceptible to ozone damage. This would allow for experiments to be shortened, and more replicates could be performed. It would also be useful to apply the coating to leaves while leaving others on the same plant uncoated while fumigating with ozone. Assuming that visible ozone damage could be detected, this would allow a controlled method of assessing if the coating could prevent visible damage.

REFERENCES

Affek H.P., Yakir D. 2003. Natural abundance carbon isotope composition of isoprene reflects incomplete coupling between isoprene synthesis and photosynthetic carbon flow. *Plant Physiol*. **131**: 1727–1736.

Ainsworth E.A., Yendrek C.R., Sitch S., Collins W.J., Emberson L.D. 2012. The effects of tropospheric ozone on net primary productivity and implications for climate change. *Annual Review of Plant Biology*. **63**: 637–661.

Arneth A., Niinemets U., Pressley S., Back J., Hari P., Karl T., Noe S., Prentice I. C., Serca D., Hickler T., Wolf A., and Smith B. 2007. Process-based estimates of terrestrial ecosystem isoprene emissions: incorporating the effects of a direct CO2-isoprene interaction. *Atmos. Chem. Phys*., **7**: 31–53.

Aschmann S.M., Atkinson R., 1994. Formation yields of methyl vinyl ketone and methacrolein from the gas-phase reaction of O3 with isoprene. *Environment Science and Technology*. **28** 1539e1542.

Atkinson R. 1994. Gas-phase tropospheric chemistry of organic compounds. *J. Phys. Chem. Ref. Data.* Monograph No. 2: 1–216.

Atkinson R. Arey J. 2003. Gas-phase tropospheric chemistry of biogenic volatile organic compounds: a review. *Atoms. Environ*. **37(2)**: 197–219.

Atkinson, R. 1997. Gas-phase tropospheric chemistry of volatile organic compounds: 1. alkanes and alkenes. *J. Phys. Chem. Ref. Data*. **26.** 215–290.

Baldocchi D., Guenther A.B., Harley P.C., Klinger L., Zimmerman P., Lamb B., Westberg H. 1995. The Fluxes and air chemistry of isoprene above a deciduous hardwood forest. *Philosophical Transactions of the Royal Society of London Series A-Mathematical Physical and Engineering Sciences*. **351**: 279–296.

Bruggemann N., Schnitzler J.P. 2002. Comparison of isoprene emission, intercellular isoprene concentration and photosynthetic performance in water-stressed oak (IQuercus pubescens Willd. and *Quercus robur* L.) saplings. *Plant Biology.* **4(4)**: 456–463.

Caemmerer S. von, Farquhar G.D., 1981. Some relationships between biochemistry of photosynthesis and the gas exchanges of leaves. *Planta.* **153(4)**: 376–387.

Cape J.N., Hamilton R., Heal M.R. 2009. Reactive uptake of ozone at simulated leaf surfaces: Implications for 'non-stomatal' ozone flux. *Atmos. Env*. **43**: 1116–1123.

Dreyfus, G.B., Schade, G.W., and Goldstein, A. H. 2002. Observational constraints on the contribution of isoprene oxidation to ozone production on the western slope of the Sierra Nevada, California, *J. Geophys. Res*. **107:** D19.

Fang, C.W., Monson, R.K., Cowling, E.B., 1996. Isoprene emission, photosynthesis, and growth in sweetgum (Liquidambar styraciflua) seedlings exposed to short- and long- term drying cycles. *Tree Physiology*. **16(4)**, 441–446.

Fares S., Loreto F., Kleist E., Wildt J. 2008. Stomatal uptake and stomatal deposition of ozone in isoprene and monoterpene emitting plants. *Plant Biol.* **10(1)**: 44–54.

Fares S., McKay M., Holzinger R., Goldstein A.H. 2010. Ozone fluxes in a Pinus ponderosa ecosystem are dominated by non-stomatal processes: Evidence from long-term continuous measurements. *Agricultural and Forest Meteorology*. **150**: 420–431.

Flexas J., Bota, J., Loreto F., Cornic G., Sharkey T. D. 2004. Diffusive and metabolic limitations to photosynthesis under drought and salinity in C3 plants. *Plant Biology*. **6**: 269–279.

Folberth G.A., Hauglustaine D.A., Lathière J., Brocheton F. 2006. Interactive chemistry in the laboratoire de morologie dynamique general circulation model: model description and impact analysis of biogenic hydrocarbons on tropospheric chemistry *Atmos. Chem. Phys*., **6:** 2273–2319.

Fowler D. et al. 2013. The global nitrogen cycle in the twenty-first century. *Phil Trans R Soc B.* 368.

Fuentes JD, Lerdau M, Atkinson R, Baldocchi D, Botteneheim JW, et al. 2000. Biogenic hydrocarbons in the atmospheric boundary layer: a review. *Bull. Am. Meteorol. Soc*. **81**: 1537–75.

Geron C., Guenther A., Sharkey T.D., Arnts R.R. 2000. Temporal variability in the basal isoprene emission factor. *Tree Physiol*., **20(12)**: pp. 799–805.

Geron C., Harley P., Guenther A. 2001. Isoprene emission capacity for US tree species. *Atmos Environ.* **35**: 3341–3352.

Glasius M., Goldstein A.H. 2016. Recent discoveries and future challenges in atmospheric organic chemistry. *Environ, Sci. Technol*. **50**: 2754–2764.

Goldstein A.H., Goulden M.L., Munger J.M., Wofsy S.C., Geron C.D. 1998. Seasonal course of isoprene emissions from a midlatitude deciduous forest. *Journal of Geophysical Research*. **103**: 31045–31056.

Grotewold, E. 2006. The genetics and biochemistry of floral pigments. *Annu. Rev. Plant Biol*. **57**: 761–780.

Guenther A, Hewitt CN, Erickson D, Fall R, Geron C, Graedel T, et al. 1995. A global model of natural volatile organic compound emissions. *Journal of Geophysical Research*. **100**: 8873–8892.

Guenther A., Karl T., Harley P., Wiedinmyer C., Palmer P.I., and Geron C. 2006. Estimates of global terrestrial isoprene emissions using MEGAN (Model of emissions of gases and aerosols from nature). *Atmos. Chem. Phys*. **6**: 3181–3210.

Guenther, A.B., Archer, S., Greenberg, J.P., Harley, P.C., Helmig, D., Klinger, L., Vierling, L., Wildermuth, M., Zimmerman, P., Zitzer, S., 1999. Biogenic hydrocarbon emissions and landcover/climate change in a subtropical savanna. *Physics and Chemistry of the Earth Part B- Hydrology Oceans and Atmosphere.* **24.6**: 659–667.

Hanson D.T., Swanson S, Graham LE, Sharkey TD. 1999. Evolutionary significance of isoprene emission from mosses. *Am. J. Bot*. **86**: 634–39.

Harley P.C., Monson R.K. & Lerdau M.T. 1999a. Ecological and evolutionary aspects of isoprene emission from plants. *Oecologia*. **118**: 109–123

Harley, P.C., Litvak, M.E., Sharkey, T.D., Monson, R.K., 1999b. Isoprene emission from velvet bean leaves—interactions among nitrogen availability, growth photon flux density, and leaf developement. Plant Physiology. 105: 279–285.

Hayes F., Williamson J. and Mills G. 2015. Species-Specific responses to ozone and drought in six deciduous trees. *Water Air Soil Pollut*. **226**: 156.

Holzinger R., Sandoval-Soto L., Rottenberger S., Crutzen P.J., Kesselmeier J. 2000. Emissions of volatile organic compounds from *Quercus ilex* L. measured by Proton Transfer Reaction Mass Spectrometry under different environmental conditions. *Jrnl. Geo. Res.* **105**:573–579.

IPCC, 2013. Climate Change 2013. The physical science basis. contribution of working group I to the fifth assessment report of the intergovernmental panel on climate change [Stocker T.F., D. Qin, G.K. Plattner, M. Tignor, S.K. Allen, J. Boschung, A. Nauels, Y. Xia, V. Bex and P.M. Midgley (eds.)]. Cambridge University Press, Cambridge, United Kingdom and New York, NY, USA, 1535 pp.

Jardine K., Abrell L., Jardine A., Huxman T., Saleska S., Arneth A., Monson R., Karl T., Loreto F., Goldstein A. 2012. Within plant isoprene oxidation confirmed by

direct emissions of oxidation products methyl vinyl ketone and methacrolein. *Global Change Biology*. **18**: 973–984.

Jardine K.J., Meyers K., Abrell L., Alves E.G., Yanez Serrano A.M., Kesselmeier J., Karl T., Guenther A., Chambers J.Q., Vickers C. 2013. Emissions of putative isoprene oxidation products from mango branches under abiotic stress. *Journal Exp. Bio.* **64**: 3697–3709.

Jetter R., Kunst L., Samuels A.L. 2006. Composition of plant cuticular waxes. In: Riederer M., Muller C. (Eds). Biology of the plant cuticle. Wiley-Blackwell. Oxford.

Johnson C.H., 2001. Endogenous timekeepers in photosynthetic organisms. *Annu. Rev. Plant Physiol. Plant Mol. Biol.* **63:** 695–728.

Jud W., Fischer L., Canaval E., Wohlfahrt G., Tissier A., Hansel A. 2016. Plant surface reactions: an opportunistic ozone defense mechanism impacting atmospheric chemistry. *Atmos. Chem. Phys*. **16**: 277–292.

Karl T. Fall R., Rosenstiel T.N., Prazeller P., Larsen B., Seufert G., et al., 2002. On-line analysis of the $13CO_2$ labeling of leaf isoprene suggests multiple subcellular origins of isoprene precursors. *Planta*. **215**: 894–905.

Kesselmeier J., Bode K., Gerlach C., Jork E.-M. 1998. Exchange of atmospheric formic and acetic acids with trees and crop plants under controlled chamber and purified air conditions. *Atmo. Env.* **32**: 1765–1775.

Lahr E.C., Schade G.W., Crossett C.C., Watson M.R. 2015. Photosynthesis emission from trees along an urban-rural gradient in Texas. *Global Change Biology*. **21**: 4221–4236.

Laisk A., Kull O., Moldau H. 1989. Ozone concentration in leaf intercellular air space is close to zero. *Plant Physiol*. **90**: 1163–1167.

Lathiere J., Hewitt C. N., and Beerling D. J. 2010. Sensitivity of isoprene emissions from the terrestrial biosphere to 20th century changes in atmospheric CO2 concentration, climate, and land use. *Glob. Biogeochem. Cycl*. **24**: G1004.

Lobell D.B. and Asner G.P. 2003. Climate and management contributions to recent trends in U.S. agricultural yields. *Science* **299**: 1032.

Loivamaki M., Louis S., Cinege G., Zimmer I., Fischbach R.J., Schnitzler J.P. 2007. Circadian rhythms of isoprene biosynthesis in grey poplar leaves. *Plant Physiol.* **143(1)**: 540–551.

Loreto F, Pinelli P, Brancaleoni E, Ciccioli P. 2004. C13 labelling reveals chloroplastic and extra-chloroplastic pools of dimethylallyl piroposphate and their contribution to isoprene formation. *Plant Physiology*. **135**: 662–669.

Loreto F., Forster A., Durr M., Cisky O., Seufert G. 1998. On the monoterpene emission under heat stress and on the increased thermotolerance of leaves of Quercus ilex L. fumigated with selected monoterpenes. *Plant, Cell & Environment.* **21**: 101–107.

Loreto F., Sharkey T.D. 1990. A gas-exchange study of photosynthesis and isoprene emission in *Quercus rubra* L. *Planta*. **182**: 523–531.

Loreto, F., Mannozzi, M., Maris, C., Nascetti, P., Ferranti, F., & Pasqualini, S. 2001. Ozone quenching properties of isoprene and its antioxidant role in leaves. *Plant Physiology*. **126(3)**, 993–1000.

Löw M., Herbinger K., Nunn A. J., Haberle K. H., Leuchner M., Heerdt C., Werner H., Wipfler P., Pretzsch H., Tausz M., Matyssek R. 2006. Extraordinary drought of 2003 overrules ozone impact on adult beech trees (Fagus sylvatica). *Trees-Structure and Function*. **20(5)**: 539–548.

Malkin T.L., Goddard A., Heard D.E., Seakins P.W., 2010. Measurements of OH and HO_2 from the gas phase ozonolysis of isoprene. *Atmos Chem. Phys.* **10**: 1441–1459.

Mgaloblishvili, M.P., Khetsuriani, N.D., Kalandadze, A.N., Sanadze, G.A., 1979. Localization of isoprene biosynthesis in poplar chloroplasts. *Plant Physiology.* **25**. 837–842.

Miller J.D., Arteca R.N., Pell E.J. 1999. Senescence-associated gene expression during ozone induced leaf senescence in Arabidopsis. *Plant Physiol.* **120(4)**: 1015–1024.

Monson R. Jones R. Rosenstiel T. and Schnitzler J. 2013. Why only some plants emit isoprene. *Plant, Cell & Environment*. **36(3):** 503–516.

Monson, R.K., Fall, R.R., 1989. Isoprene emission from aspen leaves—influence of environment and relation to photosynthesis and photorespiration. *Plant Physiology.* **90**: 267–274.

Munoz-Bertomeu J., Arrillaga I., Segura J. 2007. Essesntial oil variation within and among natural populations of Lavandula latifolia and its relation to their ecological areas. *Biochemical systematics and ecology*. **8**: 479–488.

Panek J.A. 2004. Ozone uptake, water loss and carbon exchange dynamics in annually drought-stressed Pinus ponderosa forests: measured trends and parameters for uptake modeling. *Tree Physiology*. **24**: 277–290.

Panek J.A. and Goldstein A.H. 2001. Response of stomatal conductance to drought in ponderosa pine: implications for carbon and ozone uptake. *Tree Physiology*. **21**: 337–344.

Paulot F., Crounse J.D., Kjaergaard H.G., Kroll J.H., Seinfeld J.H., and Wennberg P.O. 2009. Isoprene photooxidation: new insights into the production of acids and organic nitrates. *Atmos. Chem. Phys*. **9:** 1479-1501.

Pegoraro E, Rey A, Greenberg J, Harley P, Grace J, et al. 2004. Effect of drought on isoprene emission rates from leaves of Quercus virginiana Mill. *Atmospheric Environment.* **38**: 6149–6156.

Pell E.J., Schlagnhaufer C.D., Arteca R.N., 1997. Ozone-induced oxidative stress: Mechanisms of action and reaction. *Physiologia Plantarum*. **100**: 264–273.

Peñuelas J., Llusià J., Asensio D.A. and Munné-Bosch S. 2005. Linking isoprene with plant thermotolerance, antioxidants, and monoterpene emissions. *Plant, Cell and Environment.* **28**: 00–00.

Rao M.V., Davis K.R. 2001. The physiology of ozone induced cell death. *Planta*. **213**: 682–690.

Rosenstiel T.N., Ebbets A.L., Khatri W.C., Fall R., Monson R.K. 2004. Induction of poplar leaf nitrate reductase: a test of extrachloroplastic control of isoprene emission rate. *Plant Biol* **6**: 12–21.

Sanderson M.G., Jones C.D., Collins W.J., Johnson C.E., and Derwent R.G. 2003. Effect of climate on isoprene emissions and surface ozone levels. *Geophys. Res. Lett.* **30(18)**: 1936.

Sharkey T.D., Loreto F. 1993. Water-stress, temperature, and light effects on the capacity for isoprene emission and photosynthesis in Kudzu leaves. *Oecologia.* **95(3)**: 328–338.

Sharkey T.D., Wiberley A.E. and Donohue A.R. 2008. Isoprene emission from plants: Why and how. *Ann Bot.* **101(1)**: 5–18.

Sharkey T.D., Yeh S., Wiberley A.E., Falbel T.G., Gong D., Fernandez D.E. 2005. Evolution of the isoprene biosynthetic pathway in kudzu. *Plant Physiology*. **137**: 700–712.

Sharkey TD, Yeh S. 2001. Isoprene emission from plants. *Annual Review of Plant Physiology and Plant Molecular Biology*. **52**: 407–436.

Sharkey, T. D. 2005, Effects of moderate heat stress on photosynthesis: importance of thylakoid reactions, rubisco deactivation, reactive oxygen species, and thermotolerance provided by isoprene. *Plant, Cell & Environment*. **28**: 269–277

Singsaas EL, Laporte MM, Shi J-Z, Monson RK, Bowling DR, et al. 1999. Leaf temperature fluctuation affects isoprene emission from red oak (Quercus rubra) leaves. *Tree Physiol*. **19**: 917–24.

Singsaas EL, Sharkey TD. 1998. The regulation of isoprene emission responses to rapid leaf temperature fluctuations. *Plant Cell Environ*. **21**: 1181–88.

Tingey DT, Evans RC, Bates EH, Gumpertz ML. 1987. Isoprene emissions and photosynthesis in three ferns: the influence of light and temperature. *Physiologia Plantarum*. 69: 609–616.

Uddling J., Hogg A.J., Teclaw R.M., Carrol M.A., Ellsworth D.S. 2010. Stomatal uptake of O_3 in aspen and aspen-birch forests under free air CO_2 and O_3 enrichment. *Environmental Pollution*. **158**: 2023–2031.

Velikova V. and Loreto F. 2005. On the relationship between isoprene emission and thermotolerance in Phragmites australis leaves exposed to high temperatures and during the recovery from heat stress. *Plant, Cell and Environment.* **28**: 00–00.

Wahid A., Gelani S., Ashraf M., Foolad, M. R. 2007. Heat tolerance in plants: An overview. *Env and Exp Bio.* **61**: 199–223.

Went F.W. 1960. Blue hazes in the atmosphere. *Nature*. **187**: 641-643.

Wilkinson M.J., Owen S.M., Possell M., Hartwell J., Gould P., Hall A., Vickers C., Hewitt C.N. 2006. Circadian control of isoprene emissions from oil palm (Elaeis guineensis). *The Plant Journal.* **47**: 960–968.

Williams J, Roberts J.M., Fehsenfeld F.C., Bertman S.B., Buhr M.P., Goldan P.D., et al. 1997. Regional ozone hydrocarbons deduced from measurements of PAN, PPN, and MPAN. *Geophysical Research letters.* **24**: 1099–1102.

Wittig V.E., Ainsworth E.A., Long S.P. 2007. To what extent do current and projected increase in surface ozone affect photosynthesis and stomatal conductance of trees? A meta-analytic review of the last 3 decades of experiments. *Plant, Cell and Environment*. **30**: 1150–1162.

Wittig V.E., Ainsworth E.A., Naidu S. L., Karnosky D. F., Long, S. P. 2009. Quantifying the impact of current and future tropospheric ozone on tree biomass, growth, physiology and biochemistry: a quantitative meta-analysis. *Global Change Biology*. **15**: 396–424.